Reversibly core-crosslinked PEG-P(HPMA) micelles: Platinum coordination chemistry for competitive-ligand-regulated drug delivery

Sytze Buwalda, Benjamin Nottelet, Audrey Bethry, Robbert Jan Kok, Niels Sijbrandi, Jean Coudane

Reversibly core-crosslinked PEG-P(HPMA) micelles: Platinum coordination chemistry for competitive-ligand-regulated drug delivery

Sytze Buwalda,[a] Benjamin Nottelet,[a] Audrey Bethry,[a] Robbert Jan Kok,[b] Niels Sijbrandi,[c] Jean Coudane[a]*

[a] IBMM, Université de Montpellier, CNRS, ENSCM, Faculté de Pharmacie, 15 avenue Charles Flahault, BP14491, 34093 Montpellier cedex 5, France

[b] Department of Pharmaceutics, Utrecht Institute for Pharmaceutical Sciences, Utrecht University, Universiteitsweg 99, 3584 CG Utrecht, The Netherlands

[c] LinXis B.V., Boelelaan 1085c, Amsterdam, 1081 HV, The Netherlands

*Corresponding author. Telephone number: +33(0)4-11-75-96-97; Fax number: +33(0)4-11-75-97-28

E-mail addresses: sijtze.buwalda@umontpellier.fr; benjamin.nottelet@umontpellier.fr; audrey.bethry@univ-montp1.fr; r.j.kok@uu.nl; sijbrandi@linxispharmaceuticals.com; jean.coudane@umontpellier.fr

Abstract

Hypothesis. The presence of pendant thioether groups on poly(ethylene glycol)-poly(N(2-hydroxypropyl) methacrylamide) (PEG-P(HPMA)) block copolymers allows for platinum-mediated coordinative micellar core-crosslinking, resulting in enhanced micellar stability and stimulus-responsive drug delivery.

Experiments. A new PEG-P(HPMA) based block copolymer with pendant 4-(methylthio)benzoyl (MTB) groups along the P(HPMA) block was synthesized by free radical polymerization of a novel HPMA-MTB monomer using a PEG based macro-initiator. As crosslinker the metal-organic linker

[ethylenediamineplatinum(II)]$^{2+}$ was used, herein called *Lx*, which is a coordinative linker molecule that has been used for the conjugation of drug molecules to a number of synthetic or natural carrier systems such as hyperbranched polymers and antibodies.

Findings. The introduction of *Lx* in the micellar core results in a smaller size, a lower critical micelle concentration and a better retention of the hydrophobic drug curcumin thanks to coordination bonds between the central platinum atom of *Lx* and thioether groups on different polymer chains. The drug release from *Lx* crosslinked micelles is significantly accelerated under conditions mimicking the intracellular environment due to competitive coordination and subsequent micellar de-crosslinking. Because of their straightforward preparation and favorable drug release characteristics, core-crosslinked *Lx* PEG-P(HPMA) micelles hold promise as a versatile nanomedicine platform.

Keywords: PEG-P(HPMA); core-crosslinked micelle; coordination chemistry; controlled drug delivery; stimulus-responsive.

Introduction

Polymeric micelles, prepared from amphiphilic block copolymers, are an important and extensively studied class amongst controlled drug delivery systems because of several attractive properties. Their hydrophilic PEG corona provides them with a stealth surface, whereas their hydrophobic core acts as a depot capable of solubilizing clinically relevant doses of hydrophobic drugs.[1] However, due to their dynamic nature, classical non-crosslinked micelles may disintegrate prematurely in systemic circulation resulting from dilution in the bloodstream below the critical micelle concentration.[2] Furthermore blood components may adsorb onto the surface of nanoparticles, despite the presence of stealth PEG surface.[3] Such opsonisation of plasma proteins can trigger the activation of the complement immune system[4] or may lead to enhanced clearance of the micelles.[5] Recent developments in organic and polymer chemistry have facilitated the synthesis of block copolymers which contain functionalities allowing for

alternative interactions in order to further stabilize the micelle, in addition to hydrophobic interactions.[6] Among the different interactions, metal-ligand coordination has received increasing interest because of its high specificity and reversibility via competitive displacement. Xin et al. prepared self-assembling polymer conjugates containing a PEG chain as the hydrophilic segment, a triphenylmethyl group as the hydrophobic moiety and a catechol-bearing dopamine end group.[7] The addition of Fe^{3+} ions resulted in smaller micelles and a higher micellar stability due to coordinative core-crosslinking between Fe^{3+} and catechol groups. Under acidic conditions, the release of doxorubicin from such Fe^{3+}-catechol stabilized micelles was significantly faster compared to the release at pH 7.4 as a consequence of coordination collapse and particle de-crosslinking. The core-crosslinked micelles enabled increased doxorubicin accumulation in tumors and enhanced suppression of tumor growth in a mouse model.[7] In addition, the presence of Fe^{3+} endowed the micelles with visibility in magnetic resonance imaging (MRI). Poly(hydroxyethyl methacrylate)-poly(2-((8-hydroxyquinolin-5-yl)methoxy)ethyl methacrylate) (PHEMA-PHQ) diblock copolymers were prepared by Ren et al. via RAFT polymerization.[8] These polymers could self-assemble in ethanol into micelles having a PHEMA shell and a PHQ core. The micelles were subsequently core-crosslinked by addition of Ni^{2+}, Co^{2+} or Nd^{3+} ions resulting in coordination between the metal ions and the 8-hydroxyquinoline groups in the PHQ block. A study of the magnetic properties revealed that Ni^{2+}-crosslinked PHEMA-PHQ micelles exhibit the features of a soft ferromagnet. The group of Zhuo synthesized poly(ethylene glycol)-poly(ethylenimine)-poly(ε-caprolactone) (PEG-PEI-PCL) triblock copolymers through a condensation reaction between PEG-PEI diblock copolymer and monocarboxy-capped PCL.[9] After self-assembly of the polymers in water, the micelles were crosslinked by addition of $CuSO_4$ resulting in coordination between Cu^{2+} ions and the amino groups in the PEI block. The stabilized micelles had a higher doxorubicin loading capacity and a more sustained drug release than non-stabilized micelles. Cao et al. reported on micelle-forming poly(ethylene glycol)-poly(urethane)-poly(ethylene glycol) triblock copolymers containing a selenium atom in the backbone of the hydrophobic poly(urethane) block.[10] Micellar core-crosslinking via coordination of Pt^{2+} ions to the selenium-containing polymer resulted in a high stability at elevated

electrolyte concentrations, as the Pt-crosslinked micelles kept their size of approximately 60 nm in 2 M NaCl while the size of non-crosslinked micelles increased above 1000 nm. When dithiothreitol was added, the release of doxorubicin occurred significantly faster due to competitive coordination of the platinum cations with dithiothreitol, resulting in micellar de-crosslinking. An analogous polymer, poly(ethylene glycol)-poly(urethane)-poly(ethylene glycol) containing a tellurium atom in the poly(urethane) block, was prepared by the same research group to enable the loading of platinum based drugs such as cisplatin.[11] Micelles prepared from tellurium-containing polymers exhibited a significantly higher drug loading compared to control micelles prepared from polymers without tellurium. Via competitive coordination of biomolecules such as glutathione, the drugs could be released in a controlled manner. Furthermore, the release kinetics could be tuned by the competitive ligands involved due to their different coordination ability.

Amongst amphiphilic micelle-forming polymers, PEG-P(HPMA) based block copolymers have attracted much interest because of their biocompatibility, non-immunogenicity and the possibility for functionalization of the P(HPMA) block.[12] Because P(HPMA) itself is highly water-soluble, it can only be used as the core in polymeric micelles when it is chemically modified with hydrophobic moieties. For example, micelle-forming PEG-P(HPMA) block copolymers have been described in which the P(HPMA) block was functionalized with oligolactate,[13] benzoyl,[14] anthracene,[15] ethylcarbonate[16] and lipoic acid groups.[17] PEG-P(HPMA-benzoyl) micelles developed in the group of Hennink showed excellent stability as well as a high paclitaxel loading due to polymer-polymer and polymer-drug π-π stacking effects.[14] These micelles induced complete regression of A431 epidermoid and MDA-MB-468 breast carcinoma xenografts in mice.[18]

The examples described above clearly demonstrate the advantages of micellar stabilization by coordinative crosslinking as well as the beneficial properties of PEG-P(HPMA) based block copolymers for the formation of micelles. This led us to combine in this work these 2 promising concepts by designing PEG-P(HPMA) block copolymers with hydrophobic 4-(methylthio)benzoyl (MTB) side groups that can stabilize the micellar core via coordinative crosslinking. As crosslinker we used the

metal-organic linker [ethylenediamineplatinum(II)]$^{2+}$, herein called *Lx*, which is a coordinative linker molecule that has been used for the conjugation of drug molecules to a number of synthetic or natural carrier systems such as hyperbranched polymers and antibodies.[19-22] The properties of core-crosslinked micelles are presented and compared with those of uncrosslinked micelles. As a proof-of-principle for drug delivery applications, we demonstrate the capacity of the *Lx*-micelles to encapsulate and release curcumin, a poorly water-soluble drug exhibiting anti-cancer and anti-inflammatory properties. Lastly, the cytotoxicity of curcumin-loaded micelles is evaluated using the breast cancer cell line MCF-7. In summary, we show that core-crosslinking of PEG-P(HPMA-MTB) micelles with the *Lx* linker results in a smaller size, a lower CMC and a better retention of the hydrophobic drug. Importantly, the core-crosslinked micelles can be destabilized via competitive displacement under conditions mimicking the intracellular environment, resulting in significantly faster drug release. This study therefore confirms that the rationally designed, core-crosslinked PEG-P(HPMA-MTB) micelles are appealing as stimulus-responsive controlled drug delivery systems.

Experimental section

Materials

Dichloro(ethylenediamine)platinum(II) 99 %, silver nitrate ≥ 99.8 %, DL-1-amino-2-propanol ≥ 90 %, methacryloyl chloride ≥ 97 %, 4-(dimethylamino)pyridine ≥ 99 %, p-toluenesulfonic acid ≥ 98 %, 4-(methylthio)benzoyl chloride 95 %, triethylamine (TEA) ≥ 99 %, (aminomethyl)polystyrene, 4,4′-azobis(4-cyanopentanoic acid) (ABCPA) ≥ 98 %, poly(ethylene glycol) methyl ether (M_n = 5000 g/mol, mPEG5K), 8-anilino-1-naphthalene-sulfonic acid magnesium salt (8,1-ANS) ≥ 95 %, dithioerythritol (DTE) ≥ 99 %, dicyclohexylcarbodiimide (DCC) 99 %, curcumin ≥ 94 %, ascorbic acid ≥ 99.7 %, Tween 80, calcium hydride ≥ 97 %, potassium hydroxide 90 %, magnesium sulfate ≥ 98 % and all solvents (≥ 99.8 % pure) were obtained from Sigma-Aldrich (St-Quentin Fallavier, France). 2-Hydroxypropyl methacrylamide[23] (HPMA) and 4-(dimethylamino)pyridinium-4-toluenesulfonate[24]

(DPTS) were synthesized as reported previously. Dichloromethane (DCM) and TEA were dried over calcium hydride and potassium hydroxide, respectively, and distilled prior to use.

Synthesis

Activated *Lx* complex [platinum(II)(chlorido)(N,N-dimethylformamido)(ethylenediamine)]$(NO_3)_2$

The activated *Lx* complex was prepared according to a previously reported procedure.[20] Briefly, dichloro(ethylenediamine)platinum(II) (0.50 g, 1.50 mmol) and silver nitrate (0.25 g, 1.50 mmol) were added to DMF (77 ml) and the suspension was stirred in the dark at room temperature for 18 h. Subsequently, the mixture was filtered through 0.20 µm syringe filters to yield a clear pale green solution of the activated *Lx* linker in DMF (20 mM).

N-(2-(4-(methylthio)benzoyl)oxypropyl)methacrylamide (HPMA-MTB)

A solution of 4-(methylthio)benzoyl chloride (1.83 g, 9.8 mmol) in 15 ml DCM was added dropwise to a solution of HPMA (1.63 g, 11 mmol) and TEA (1.60 ml, 11 mmol) in 5 ml DCM under stirring. The reaction was allowed to proceed for 96 h in the dark at room temperature in an argon atmosphere. The reaction mixture was filtered, washed with brine and dried with magnesium sulfate. The resulting solution was then stirred for 24 h in the presence of (aminomethyl)polystyrene. The resin was removed by filtration and HPMA-MTB was obtained as a brown solid after evaporation of DCM in vacuo. Yield: 1.50 g (42 %). ^{1}H NMR (300 MHz, $CDCl_3$, δ): 7.92 and 7.26 (d, 4H, aromatic protons), 6.24 (br s, 1H, CO−N*H*−CH_2), 5.65 and 5.29 (s, 2H, C*H*$_2$=C), 5.28 (m, 1H, CH_2−C*H*(CH_3)−O), 3.60 (m, 2H, NH−C*H*$_2$−CH), 2.52 (s, 3H, −S−C*H*$_3$), 1.93 (s, 3H, C*H*$_3$−C=C), 1.40 (d, 3H, CH_2−CH(C*H*$_3$)−O).

$(PEG)_2$-ABCPA macro-initiator

$(PEG)_2$-ABCPA was synthesized following a previously reported procedure.[25] Briefly, ABCPA (0.11 g, 0.4 mmol), mPEG5K (4.00 g, 0.8 mmol) and DPTS (38 mg, 0.13 mmol) were dissolved in 22 ml of a mixture of DCM and dry DMF (10/1 v/v). After cooling the solution in an ice bath, a solution of DCC

(0.25 g, 1.2 mmol) in 5 ml DCM was added dropwise under stirring. The reaction mixture was allowed to warm to room temperature and stirred for 18 hours in an argon atmosphere. The mixture was filtered, concentrated and precipitated in a large excess of cold diethyl ether. $(PEG)_2$-ABCPA was collected by filtration and dried overnight in vacuo to give a white powder. Yield: 3.35 g (85 %). ^{1}H NMR (300 MHz, $CDCl_3$, δ): 4.25 (m, 4H, terminal PEG protons), 3.63 (m, 1020H, PEG protons), 3.37 (s, 6H, C*H*$_3$−O−CH_2−CH_2), 2.30-2.64 (br, 8H, C−C*H*$_2$−C*H*$_2$−C=O), 1.66 and 1.72 (s, 6H, C−C*H*$_3$). SEC: M_n 12700 g/mol, PDI 1.17.

PEG-P(HPMA-MTB) diblock copolymer

$(PEG)_2$-ABCPA (0.54 g, 53 μmol) and HPMA-MTB (0.35 g, 1.2 mmol) were dissolved in 3.5 ml of methanol. The solution was stirred at 70 °C under reflux for 18 h in an argon atmosphere. After removal of the methanol by rotary evaporation, the crude product was dissolved in DCM and precipitated in a large excess of cold diethyl ether. PEG-P(HPMA-MTB) was obtained by filtration and dried overnight in vacuo to give an off-white powder. Yield: 0.70 g (80 %). ^{1}H NMR (300 MHz, DMSO-d_6, δ): 7.83 and 7.27 (br, 36H, aromatic protons), 4.98 (br, 9H, NH-CH_2-C*H*(CH_3)-O-(MTB)), 3.50 (m, 510H, PEG protons), 3.23 (s, 3H, C*H*$_3$−O−CH_2−CH_2), 3.14 (br, 18H, NH-C*H*$_2$-CH), 2.47 (s, 27H, −S−C*H*$_3$), 1.5 - 2.0 (br, 18H, backbone methylene protons), 1.20 (br, 27H, NH-CH_2-CH(C*H*$_3$)-O-(MTB)), 0.5 - 1.0 (br, 27H, backbone methyl protons). SEC: M_n 11300 g/mol, PDI 1.35.

Characterization

^{1}H, ^{13}C and ^{195}Pt NMR spectra were recorded on a Bruker AMX 300 MHz, a Bruker Avance III HD 400 MHz and a Bruker MSL 400 MHz spectrometer, respectively, at 25 °C. Compounds were dissolved in $CDCl_3$, DMSO-d_6 or D_2O at a concentration of 15 mg/ml. As a standard, residual internal $CHCl_3$ (δ 7.26 in case of ^{1}H NMR, δ 77.16 in case of ^{13}C NMR) or DMSO (δ 2.50) was used. ^{195}Pt NMR spectra were referenced externally to Na_2PtCl_6 in D_2O (0 ppm).

The number-average and weight-average molar masses (M_n and M_w, respectively) and polydispersity (PDI, M_w/M_n) of the polymers were determined by size exclusion chromatography (SEC) using a Viscotek GPCmax VE2100 liquid chromatograph equipped with a Viscotek VE3580 refractive index detector operating at 35 °C. Tetrahydrofuran was used as the eluent and the flow rate was set up at 1.0 ml/min. Two LT5000L 300 x 7.8 mm columns operating at 29 °C were used. Molecular weights were determined using the conventional narrow standard calibration technique with polystyrene standards (600-1000000 g/mol).

FTIR spectra were recorded using a Perkin-Elmer Spectrum 100 FTIR spectrometer.

Preparation and characterization of micelles

For the preparation of 1 ml of a 0.5 w/v % solution of PEG-P(HPMA-MTB) micelles core-crosslinked via the *Lx* linker (*Lx* PEG-P(HPMA-MTB) micelles), typically 5 mg PEG-P(HPMA-MTB) was dissolved in 175 µl of activated *Lx* linker DMF solution (0.5 equivalents of *Lx* relative to MTB groups). The conjugation reaction was allowed to proceed at 37 °C for 48 h, followed by evaporation of DMF under reduced pressure. The polymer-linker conjugates were subsequently dissolved in 2 ml of a mixture of acetone and water (1/1 v/v) to allow formation of core-crosslinked micelles via coordination chemistry, followed by evaporation of the acetone under atmospheric pressure for 48 h. Non-*Lx* PEG-P(HPMA-MTB) micelles (0.5 w/v %) were typically prepared by adding 1 ml of a polymer solution in THF (5 mg/ml) dropwise into 1 ml of water under magnetic stirring, followed by evaporation of THF under atmospheric pressure for 48 h.

The critical micelle concentration (CMC) of the PEG-P(HPMA-MTB) block copolymer was determined in the presence and absence of the *Lx* linker using 8,1-ANS as a fluorescent probe. Polymer solutions were prepared at different concentrations as described above. Polymer solution (200 µl) was pipetted into the wells of a black 96-well plate (Greiner), followed by 2 µl of a 5 mM 8,1-ANS solution in water. The plate was incubated for 18 h in the dark, after which the fluorescence was measured using a BMG Labtech Clariostar plate reader. The excitation and emission wavelengths were 355 and 520 nm,

respectively. The fluorescence intensity was plotted against the polymer concentration and the intercept of the extrapolated straight lines was taken as the CMC.

Dynamic light scattering (DLS) of non-*Lx* and *Lx* PEG-P(HPMA-MTB) micellar solutions (0.5 w/v % in water) was performed to determine aggregate sizes. Experiments were carried out at 25 °C using a Malvern Zetasizer Nano ZS, a laser wavelength of 633 nm and a scattering angle of 173º. The sample positioning, attenuation selection and the measurement duration were run in automatic mode. Each measurement was the result of 10-15 test runs.

The morphology of non-*Lx* and *Lx* PEG-P(HPMA-MTB) micelles was evaluated by transmission electron microscopy (TEM). One drop of a micellar solution in water was applied to a carbon-coated copper grid and the water was evaporated overnight in air. Images were obtained with a JEOL 1200 EXII-120 kV transmission electron microscope equipped with an EMSIS Quemesa camera.

Preparation of curcumin-loaded micelles

For the preparation of a typical batch of curcumin-loaded *Lx* PEG-P(HPMA-MTB) micelles (polymer concentration 0.5 w/v %), 25 mg PEG-P(HPMA-MTB)-*Lx* conjugate (containing 20 mg polymer) was dissolved in 7 ml of a mixture of acetone and water (3/4 v/v) followed by addition of 1 ml of a curcumin solution in acetone (3 mg/ml) under magnetic stirring at 1000 rpm. The stirring was continued for 10 min, followed by evaporation of the acetone under atmospheric pressure for 48 h. The resulting curcumin-loaded micellar solution was filtered through 0.45 μm syringe filters to remove precipitated, unincorporated curcumin, yielding 4 ml of a clear, orange micellar solution.

Curcumin-loaded non-*Lx* PEG-P(HPMA-MTB) micelles (polymer concentration 0.5 w/v %) were typically prepared by adding 1 ml of a polymer THF solution (20 mg/ml) dropwise into 4 ml of water under magnetic stirring at 1000 rpm, followed by addition of 1 ml of a curcumin solution in acetone (3 mg/ml). The stirring was continued for 10 min, followed by evaporation of the acetone and THF under atmospheric pressure for 48 h. The resulting curcumin-loaded micellar solution was filtered through 0.45 μm syringe filters to remove precipitated, unincorporated curcumin, yielding 4 ml of a turbid,

yellow micellar solution. The initial curcumin feed was 15 wt % relative to the polymer mass for both types of micelles.

Determination of drug loading and encapsulation efficiency

Drug loading (DL) and encapsulation efficiency (EE) were determined by adding 0.25 equivalent of acetone (v/v) to freshly prepared micellar solutions to break down the micelles and dissolve the initially loaded curcumin. Quantification was subsequently performed using a BMG Labtech Clariostar plate reader at 425 nm with reference to a calibration curve of curcumin in a mixture of acetone and water (1/4 v/v). The DL and EE were calculated based on the following formulae:

$$DL\ (\%) = 100 \times (M_C) / (M_P + M_C)$$

$$EE\ (\%) = 100 \times (M_C) / (M_{Ci})$$

with M_C = mass of curcumin in micelles, M_P = mass of copolymer and M_{Ci} = mass of curcumin initially added during the preparation of micelles.

In vitro drug release assay

The release of curcumin from micelles was measured in water containing 0.1 w/v % Tween 80 and 0.0015 w/v % ascorbic acid at 37 °C under constant orbital shaking at 150 rpm. Tween is regularly used to provide water-solubility to curcumin in such assays.[26] Ascorbic acid is a naturally occurring antioxidant, which is used to avoid the degradation of the released curcumin.[27] In a typical release study, 0.75 ml of curcumin-loaded micellar solution was injected in a dialysis device (Spectra-Por Float-A-Lyzer G2, MWCO 3.5 kDa) that was subsequently immersed in 15 ml of release medium at 37 °C in the dark. At specific time points, the entire release medium was removed and replaced with 15 ml fresh medium. Collected samples were diluted with 0.25 equivalent (v/v) of acetone and analyzed at 425 nm with reference to a calibration curve of curcumin in a mixture of acetone and water (1/4 v/v). The amount of released curcumin (R_C) was calculated based on the following formula:

$$R_C\ (\%) = 100 \times (M_{RC}) / (M_C)$$

with M_{RC} = mass of released curcumin and M_C = mass of curcumin in micelles.

To mimick the intracellular environment, 10 mM of dithioerythritol (DTE) was added to the release medium for selected experiments.

In vitro cell experiments

Cell culture

Human breast cancer cells (MCF-7) were purchased from ECACC. The cells were maintained in DMEM-F12 supplemented with fetal bovine serum (5 v/v %) and 1 % penicillin/streptomycin at 37 °C in a humidified incubator containing 5 % CO_2. MCF-7 cells were tested to be free of mycoplasma.

Cytotoxicity of unloaded micelles

The cytotoxicity of unloaded micelles was assessed in MCF-7 cells using the lactate dehydrogenase activity assay (LDH assay, Pierce). For this assay, cells were seeded in a white 96-well plate in amounts of $1 \cdot 10^4$ cells per well and allowed to attach overnight. They were then treated with unloaded non-*Lx* PEG-P(HPMA-MTB) micelles or unloaded *Lx* PEG-P(HPMA-MTB) micelles (polymer concentrations 0.03 and 0.14 w/v % in cell medium, respectively). Cell viability was assessed at 1 h, 2 h, 4 h, 6 h and 24 h using the LDH assay according to the manufacturer's instructions. Briefly, equal amounts of cell supernatant and LDH reaction mixture were mixed and incubated for 30 minutes at room temperature. Subsequently, the absorbance was read at 490 nm using a BMG Labtech Clariostar plate reader. Lysis buffer and cell culture medium were used as positive and negative control, respectively. The micellar formulations were prepared in distilled water and subsequently diluted using cell medium under laminar flowhood conditions to achieve the indicated concentrations and guarantee the absence of bacterial contaminations.

Bioactivity of curcumin-loaded micelles

The cytotoxicity of the micelles was assessed in MCF-7 cells using the CellTiter Glo assay (Promega). For this assay, cells were seeded in a white 96-well plate in amounts of $1 \cdot 10^4$ cells per well and allowed to attach overnight. They were then treated with free curcumin (0.03 µg/ml in cell culture medium), free curcumin which was solubilized with DMSO as a co-solvent (8 µg/ml dissolved in cell culture medium containing 0.1 v/v % DMSO), curcumin-loaded non-*Lx* PEG-P(HPMA-MTB) micelles (curcumin concentration 50 µg/ml, polymer concentration 0.03 w/v % in cell medium) or curcumin-loaded *Lx* PEG-P(HPMA-MTB) micelles (curcumin concentration 8 and 50 µg/ml, polymer concentration 0.01 and 0.14 w/v % in cell medium respectively). Cell culture medium containing 0.1 v/v % DMSO or medium only was used as a control. Cell viability was assessed at 1 h, 2 h, 4 h, 6 h, 24 h, 48 h and 72 h using the CellTiter Glo luminescent cell viability assay according to the manufacturer's instructions. Briefly, CellTiter-Glo reagent was added in each well with a volume equal to the volume initially present in each cell culture well. After 10 minutes incubation at room temperature, luminescence was recorded on a BMG Labtech Clariostar. The luminescent signal is proportional to the amount of ATP present in cell medium after cell lysis and hence to the number of cells in the well. The micellar formulations as well as the aqueous solution of free curcumin were prepared in distilled water and subsequently diluted using cell medium under laminar flowhood conditions to achieve the indicated concentrations and guarantee the absence of bacterial contaminations.

Cellular uptake

The cellular uptake of curcumin-loaded micelles was assessed in MCF-7 cells. Briefly, $3 \cdot 10^4$ cells were seeded into each well of a Lab-Tek II chamber slide 8-well and incubated at 37 °C in 5 % CO_2 for 3 days. Cells were then treated for 90 min with curcumin-loaded non-*Lx* PEG-P(HPMA-MTB) micelles or curcumin-loaded *Lx* PEG-P(HPMA-MTB) micelles. The curcumin concentration was 50 µg/ml for both formulations. To evaluate the cellular uptake, cell medium was replaced and observations were

done directly employing an inverted fluorescence microscope (Leica DM IRB) using a magnification of 40x (excitation 488 nm, emission 525 nm).

Results and Discussion

Synthesis and characterization of PEG-P(HPMA-MTB) block copolymers with pendant 4-(methylthio)benzoyl groups

Amphiphilic block copolymers based on PEG and hydrophobized P(HPMA) represent an excellent basis for long-acting micelles because of their hydrolytic stability and biocompatibility. Two main strategies have been reported for the preparation of the hydrophobically modified P(HPMA) block: polymerization of functionalized HPMA or post-polymerization functionalization of pre-formed P(HPMA). The post-polymerization strategy allows for preparation and characterization of the polymer backbone prior to functionalization, but at the possible cost of a limited functional group density and a change in the chemical and physical state of the polymer depending on the post-polymerization reaction conditions. The functionalized monomer strategy, on the other hand, may yield polymers with a high number of functional groups along the P(HPMA) chain. For the present micellar system, we selected the functionalized monomer strategy in order to achieve a high number of HPMA side groups capable of forming coordination bonds with the *Lx* linker, which potentially leads to a high level of core-crosslinking. A new monomer, N-(2-(4-methylthio)benzoyloxypropyl) methacrylamide (HPMA-MTB), was synthesized by reaction of 4-(methylthio)benzoyl chloride with N-(2-hydroxypropyl) methacrylamide (Figure 1). This monomer contains a thioether group, which has been shown to form robust, yet reversible coordinative bonds with the platinum atom in the *Lx* linker.[20]

After purification, the product was obtained in 42 % yield as a light brown solid. Its structure was confirmed by ^{1}H and ^{13}C NMR spectroscopy (Figures S1 and S2, respectively).

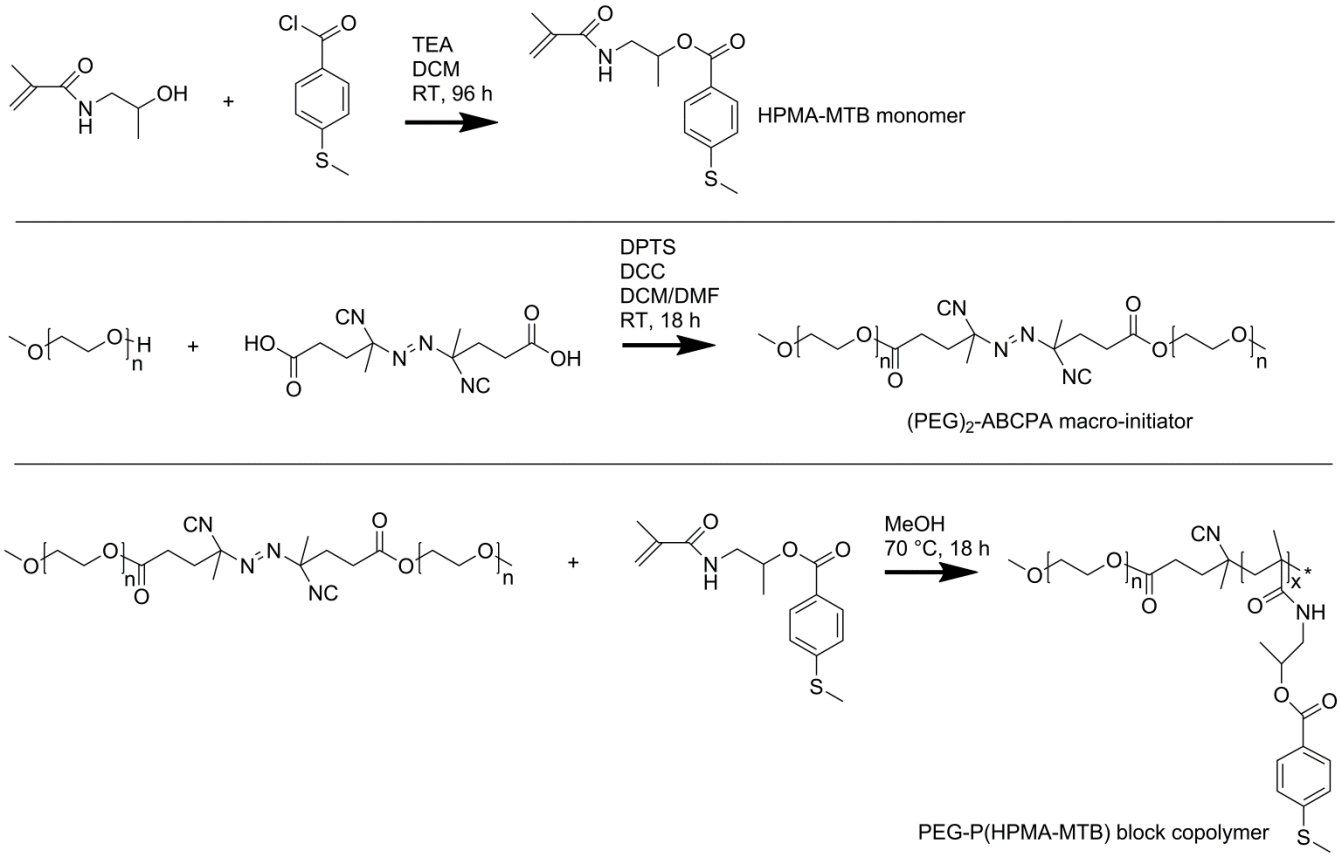

Figure 1. Synthesis scheme for the preparation of HPMA-MTB monomer (top panel), $(PEG)_2$-ABCPA macro-initiator (middle panel) and PEG-P(HPMA-MTB) block copolymer (bottom panel).

For the synthesis of amphiphilic AB block copolymers composed of PEG5K and a P(HPMA-MTB) block, we employed free radical polymerization using a monomethoxy-PEG substituted macro-initiator (Figure 1). $(PEG)_2$-ABCPA was prepared following a previously reported procedure and its structure confirmed by ^{1}H NMR (Figure S3).[25] The SEC trace of $(PEG)_2$-ABCPA (Figure S4) shows the presence of a small molecular weight shoulder that has the same retention time as PEG5K, which indicates that a small amount of PEG5K homopolymer was present in $(PEG)_2$-ABCPA. The PEG5K probably originates from the macroinitiator synthesis, i.e. PEG5K that was either not coupled to ABCPA or PEG5K that was coupled to only one of the two available COOH groups of ABCPA, as shown previously.[14] Separation of the PEG5K homopolymer and $(PEG)_2$-ABCPA (10 kg/mol) via commonly used separation techniques, which are based on differences in molecular weight, is very challenging. For

example, methods such as preparative chromatography and dialysis have been reported to be impractical, expensive and not efficient.[28]

For the synthesis of PEG-P(HPMA-MTB), the ratio between HPMA-MTP and $(PEG)_2$-ABCPA in the feed composition was set at 22/1 (mol/mol). By comparing the C=C stretch absorption peak at 1665 cm^{-1} (relative to the aromatic C-H bending absorption peak at 760 cm^{-1}) in FTIR spectra of HPMA-MTB and the crude reaction mixture after polymerization, the conversion of HPMA-MTB was estimated to be 90 %, which is in good accordance with previous research concerning free radical polymerization of functionalized HPMA monomers.[14, 29] Because thermal decomposition of every $(PEG)_2$-ABCPA leads to the formation of two PEG macroradicals, this corresponds to a theoretical degree of polymerization (DP) of approximately 10 for the P(HPMA-MTB) block. The polymer was obtained in high yield after purification (80 %). By comparing the ^1H NMR integrals of the peaks corresponding to the aromatic protons in the HPMA-MTB units and the main chain protons of PEG (Figure 2), an average DP of 9 was calculated for the P(HPMA-MTB) block (copolymer M_n 7500 g/mol). Similar to $(PEG)_2$-ABCPA, the SEC trace of PEG-P(HPMA-MTB) (Figure S4) shows the presence of a small molecular weight population with the same retention time as PEG5K. Part of this population originates from PEG5K that was not coupled to ABCPA. In addition, primary radical recombination and chain transfer, which decrease the initiator efficiency, may also give rise to PEG5K homopolymers. This chain termination during polymerization can be suppressed by applying controlled radical polymerization techniques, including reversible addition-fragmentation chain transfer (RAFT) polymerization[30] and atom transfer radical polymerization (ATRP),[31] which are the subject of current investigations. SEC analysis indicated a PDI of 1.35 for PEG-P(HPMA-MTB), which is relatively low for a polymer obtained by free radical polymerization. Similar values have been reported previously for PEG-P(HPMA) type diblock copolymers which were prepared via the $(PEG)_2$-ABCPA macroinitiator route.[32] The low PDI values may result from the relatively low DP of the polymers. PDIs of PHPMA based block copolymers obtained by controlled radical polymerizations may be even lower.[33]

Because of the presence of PEG5K homopolymer, it is likely that calculation of the M_n of PEG-P(HPMA-MTB) via ^1H NMR integration (7.5 kg/mol) results in underestimation of the M_n. An additional indication is found in the M_n calculated via SEC, which gives a value of 11.3 kg/mol. Although the molecular weight of PEG-P(HPMA-MTB) was determined using the conventional narrow standard calibration technique with polystyrene standards, which may result in overestimation of the M_n,[34] it seems therefore plausible that the actual DP of the P(HPMA-MTB) block is larger than the theoretical DP of 10. Overall, the mixture of different polymers including diblock copolymers and homopolymers can form mixed micelles in aqueous solution, as shown by DLS analysis of the micelles (vide supra) indicating that there is only one size population with a relatively low PDI. Although the synthesis of PEG-P(HPMA) type block copolymers via the $(PEG)_2$-ABCPA macroinitiator route may result in multimodal SEC distributions, these polymers have successfully been used for various biomedical applications including drug delivery[35] and imaging.[29] Moreover, this route is straightforward and cost-effective as it avoids the use of chain transfer agents, which may be costly and may require extensive purification due to toxicity and coloration issues (e.g. certain RAFT agents).

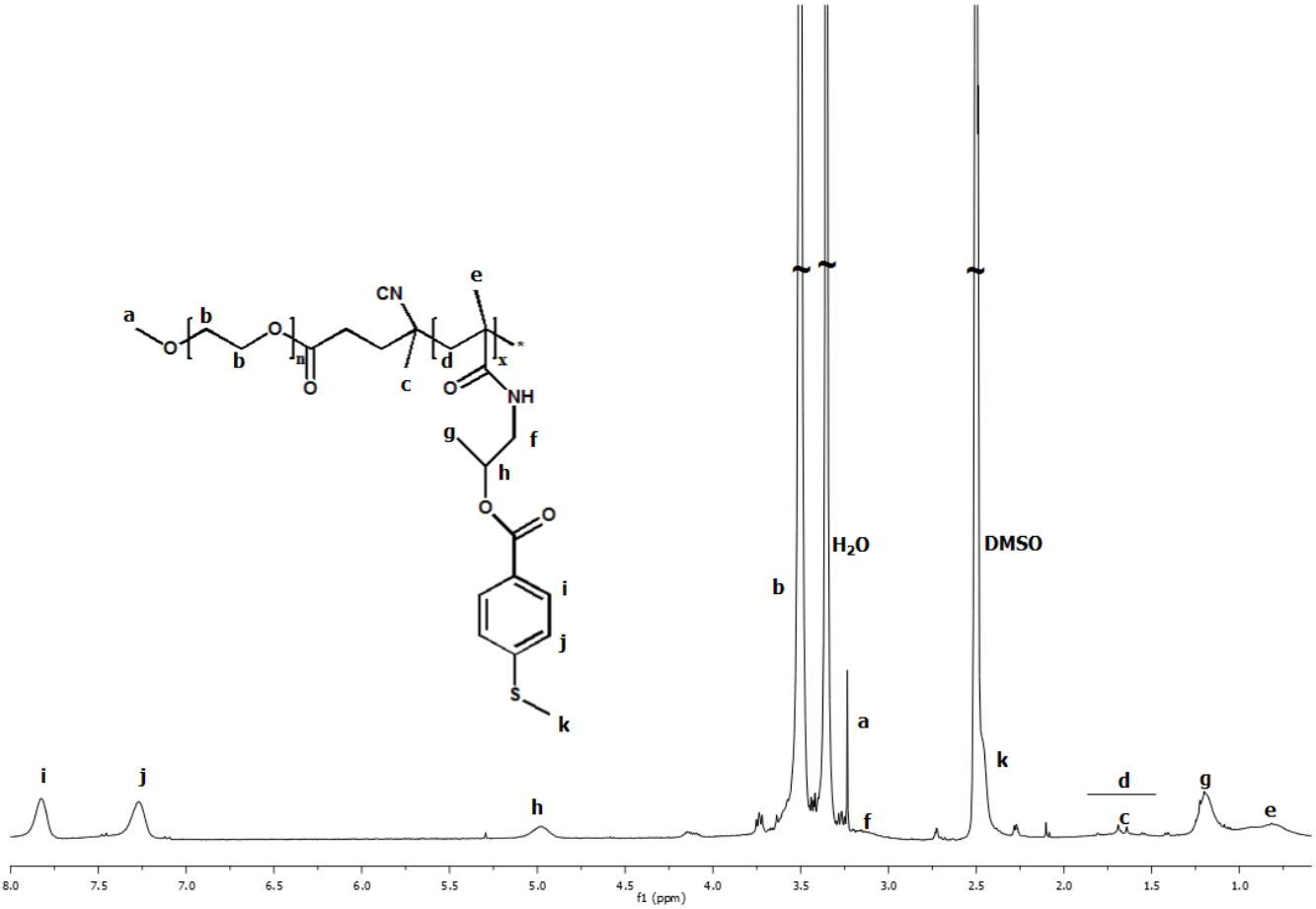

Figure 2. ^{1}H NMR spectrum of PEG-P(HPMA-MTB). Solvent: DMSO-d_6. Signals corresponding to the amide protons and the main chain protons between the PEG and P(HPMA-MTB) blocks may not be visible because of overlap with other signals.

Preparation of micelles

Previously PEG-P(HPMA-Bz) block copolymers bearing pendant benzoyl groups along the P(HPMA) block have been shown to self-assemble in water to form micelles with a hydrophilic PEG corona and a P(HPMA) core which is stabilized by π-π stacking between the aromatic groups.[14] Following a similar self-assembly approach, PEG-P(HPMA-MTB) micelles were initially prepared in the absence of the *Lx* coordinative linker by adding a THF solution of polymer into water followed by evaporation of THF (Figure 3, top panel). In view of previous literature and the structural similarity between PEG-P(HPMA-Bz) and PEG-P(HPMA-MTB) it is our belief that π-π stacking plays an important role in PEG-P(HPMA-MTB) micelles. To further investigate and confirm the π-π stacking

additional experiments are needed and underway. The critical micelle concentration (CMC) of the PEG-P(HPMA-MTB) block copolymer in aqueous solution was found to be 0.03 w/v % using a dye solubilization method employing the hydrophobic fluorescent probe 8,1-ANS (Figure S5). This value is higher than the previously reported CMC of PEG-P(HPMA-Bz) (0.0001 w/v %),[14] likely because of the substantially shorter P(HPMA) block length in case of PEG-P(HPMA-MTB) (3 vs. 17 kg/mol), resulting in less hydrophobic interactions and possibly less π-π stacking effects. Using dynamic light scattering (DLS) D_H in 0.5 w/v % PEG-P(HPMA-MTB) aqueous solutions was found to be 160 nm with a PDI of 0.18 (Figure 4).

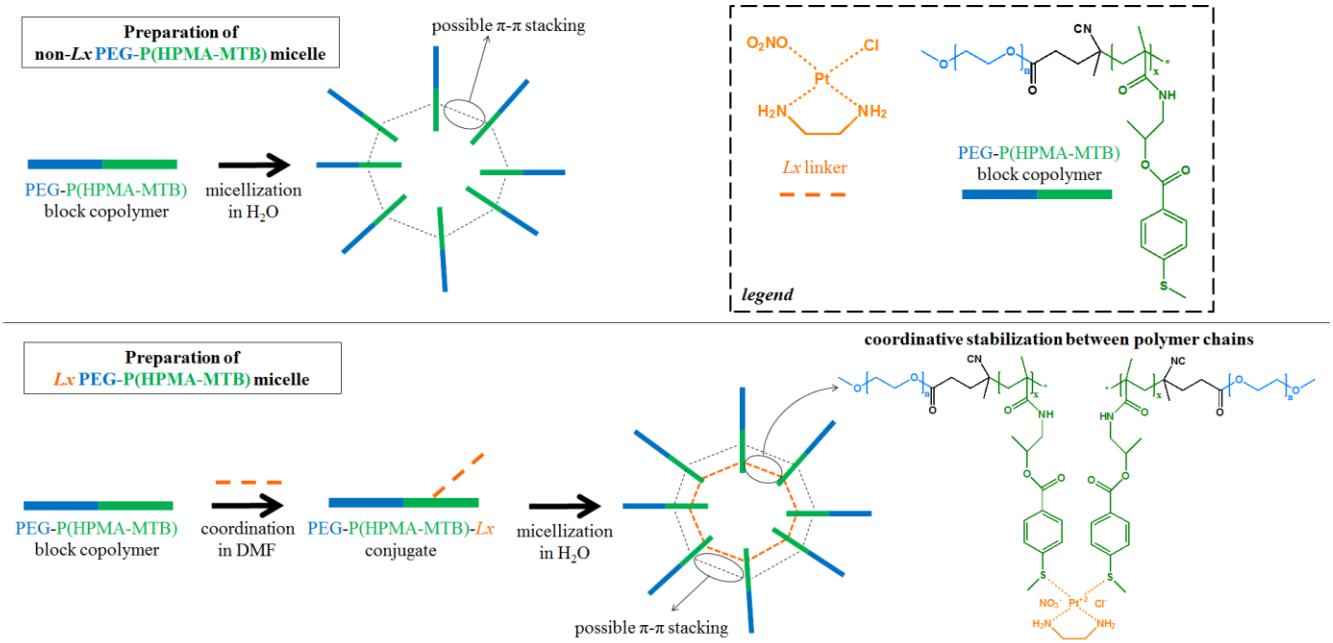

Figure 3. Schematic representation of the formation of non-*Lx* PEG-P(HPMA-MTB) micelles (top panel) and *Lx* PEG-P(HPMA-MTB) micelles (bottom panel).

With the aim of providing additional stability to the micellar core, next to hydrophobic interactions and possibly π-π stacking,[14] we subsequently introduced the coordinative *Lx* linker in the core of PEG-P(HPMA-MTB) micelles. Although covalent core-crosslinking can also provide stable micelles, it may be practically challenging because it requires additional reaction and purification steps. For this reason we selected coordinative core-crosslinking as it can be applied via a straightforward method under mild

conditions, while still offering robust crosslinks in the micellar core. Importantly, coordinative core-crosslinks can be broken via competitive coordination by e.g. glutathione, which offers the possibility of stimulus-responsive drug release. Previously the *Lx* linker has been used for the attachment of various drug molecules to macromolecular carrier systems including antibodies[19, 20] and polymers.[21] In these cases, the central platinum atom binds the functional moiety to the carrier molecule via coordination sites such as nitrogen and sulfur atoms with free electron pairs, while the other two coordination sites of platinum are made up permanently by an ethylenediamine bridge, which is a strong bidentate ligand that cannot be readily replaced by the mentioned monodentate ligands. On the other hand, the nitrate and chloride ligands that are initially present on *Lx* are weak ligands for platinum(II) and are readily replaced.[19, 20] In the present work we employ the *Lx* linker for the first time to act as a linker between two polymer molecules.

Lx crosslinked micelles were prepared by first coordinating the pendant thioether groups in the P(HPMA-MTB) block with *Lx* linker in a 2:1 ratio in DMF, resulting in substitution of the nitrate ligand on *Lx* by one thioether group (Figure 3, bottom panel). During this process, no gel formation in DMF was observed, demonstrating that no premature crosslinking took place. After DMF evaporation, the polymer-linker conjugates were dissolved in a mixture of acetone and water (1/1 v/v) as they were not soluble in water or any volatile organic solvent alone. The evaporation of the acetone induced the micellization of the polymer-linker conjugates in water, facilitating substitution of the second ligand of *Lx*, the chloride ligand, by a second thioether group on a different P(HPMA-MTB) chain in the hydrophobic core, resulting in coordinative crosslinks between the polymer molecules constituting the micelle. Using this straightforward preparation method, the CMC of *Lx* crosslinked micelles (termed *Lx* PEG-P(HPMA-MTB) micelles from here on) was found to be 0.009 w/v % (Figure S5), which is lower than the CMC of non-*Lx* PEG-P(HPMA-MTB) micelles (0.03 w/v %). The tendency of the polymers to form micelles at lower concentrations in the presence of *Lx* linker is a strong indication for *Lx* mediated coordinative core-crosslinking. Moreover, DLS measurements showed a shift of the micellar size to

smaller dimensions upon the introduction of *Lx* from 160 nm to 60 nm (Figure 4, PDI of 0.26), reflecting a more condensed core in the micelles due to the coordinative crosslinking. TEM images (Figure S6) demonstrated the presence of spherical micelles with a diameter of approximately 120 nm (non-*Lx* PEG-P(HPMA-MTB) micelles) and 60 nm (*Lx* PEG-P(HPMA-MTB) micelles), which confirms the clear size difference found in the DLS experiments (Figure 4).

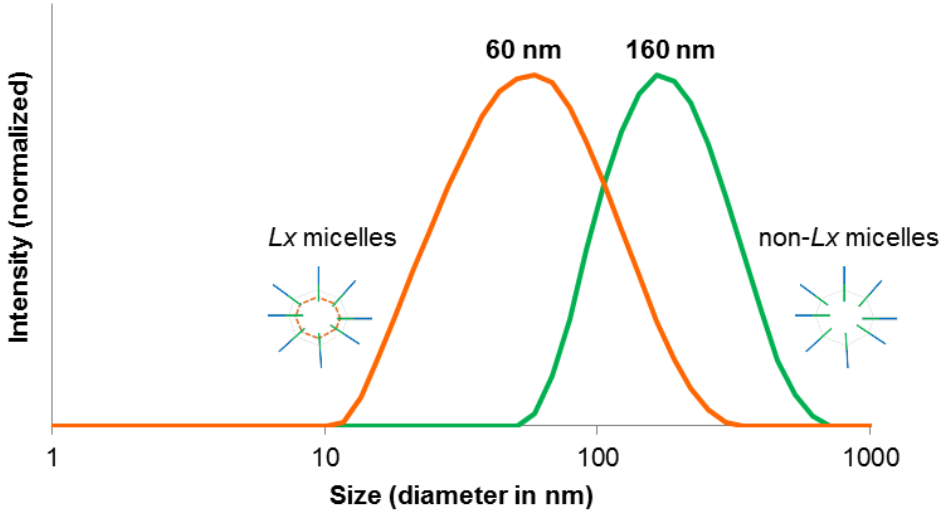

Figure 4. Aggregate size distributions of non-*Lx* and *Lx* PEG-P(HPMA-MTB) micellar solutions (0.5 w/v % in water) at 25 °C.

To further investigate the coordinative crosslinking in the micellar core, a *Lx* PEG-P(HPMA-MTB) micellar solution prepared in D_2O was analyzed by ^{195}Pt NMR spectroscopy. One main peak is observed at -3160 ppm (Figure S7). It is known from literature that the ^{195}Pt NMR chemical shift of Pt(II) compounds with a PtN_2S_2 coordination sphere is located between -3150 and -3250 ppm.[36, 37] Therefore, the peak at -3160 ppm likely relates to Pt which is coordinated by the ethylenediamine bridge and 2 thioether groups. Although the existence of coordination between thioether groups on the same polymer cannot be excluded, these ^{195}Pt NMR measurements are additional evidence for the existence of coordinative crosslinks between the polymer molecules constituting the micelle (Figure 3, bottom panel).

Curcumin incorporation and release

Curcumin is a naturally occurring low molecular weight compound which is extracted from the Curcuma Longa plant. Curcumin has various pharmacological activities, such as anti-inflammatory, anti-oxidant, anti-bacterial, anti-virus and anti-cancer effects. However, significant disadvantages of curcumin are its low water solubility (11 ng/ml[38]) and its poor stability under physiological conditions. Furthermore, the absorption of curcumin in the gastro-intestinal tract is minimal and it is toxic at high concentrations. With the aim of improving its solubility and stability and making the drug applicable via intravenous injection, curcumin was loaded in non-*Lx* PEG-P(HPMA-MTB) and *Lx* PEG-P(HPMA-MTB) micelles via the self-assembly method. Figure 5 clearly shows the solubilizing effect of the micelles. In the absence of copolymer, curcumin is almost insoluble as shown in Figure 5A where precipitated curcumin is visible at the bottom of the vial and only slight coloration of the solution appears. In contrast, encapsulation of curcumin in the hydrophobic core of non-*Lx* PEG-P(HPMA-MTB) and *Lx* PEG-P(HPMA-MTB) micelles (Figure 5B and 5C) yields homogenous solutions. The incorporation of curcumin in the micelles did not have an effect on the micellar size, as the D_H of non-*Lx* and *Lx* PEG-P(HPMA-MTB) micelles remained 160 and 60 nm, respectively (Table 1). This size difference is clearly visible in Figure 5, where *Lx* PEG-P(HPMA-MTB) micelles yield a clear solution whereas the non-*Lx* PEG-P(HPMA-MTB) micellar solution is turbid. Incorporation of curcumin in *Lx* PEG-P(HPMA-MTB) micelles results in a slight color change of curcumin, likely due to interaction of its conjugated electron system with the platinum. However, after release from the micelles the curcumin got back its original color (data not shown).

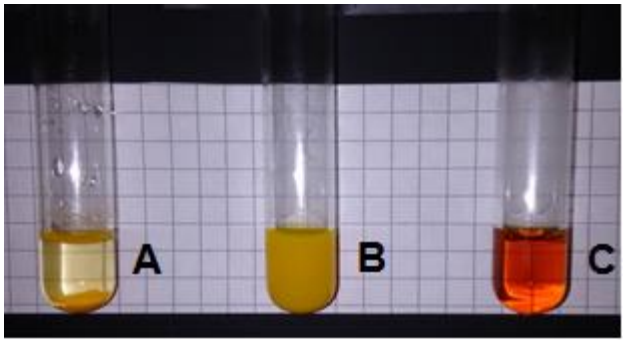

Figure 5. Dispersion of curcumin in water (A). Curcumin-loaded non-*Lx* PEG-P(HPMA-MTB) micelles (B). Curcumin-loaded *Lx* PEG-P(HPMA-MTB) micelles (C).

Non-*Lx* PEG-P(HPMA-MTB) micelles exhibit a very high EE of 97 %, which may be explained by the presence of hydrophobic interactions and possibly π-π stacking[14] between the pendant MTB groups of the polymer and the aromatic groups of curcumin. Similar high EE and DL were reported for the incorporation of curcumin in PEG-P(HPMA-Bz) block copolymers bearing pendant benzoyl groups along the P(HPMA) block.[35] Since the curcumin loading for the *Lx* PEG-P(HPMA-MTB) micelles was performed after the core-crosslinking, the latter may have acted as a physical barrier for the drug to reach the micellar core. The resulting slow kinetics of the curcumin diffusion into the core may explain the lower EE of 35 % for the *Lx* PEG-P(HPMA-MTB) micelles.

Table 1. Size, encapsulation efficiency (EE) and drug loading (DL) for curcumin-loaded non-*Lx* and *Lx* PEG-P(HPMA-MTB) micelles.

Micelle type	DLS		DL (%)	EE (%)
	D_H (nm)	PDI		
Non-*Lx* PEG-P(HPMA-MTB)	160	0.13	13	97
Lx PEG-P(HPMA-MTB)	60	0.17	5	35

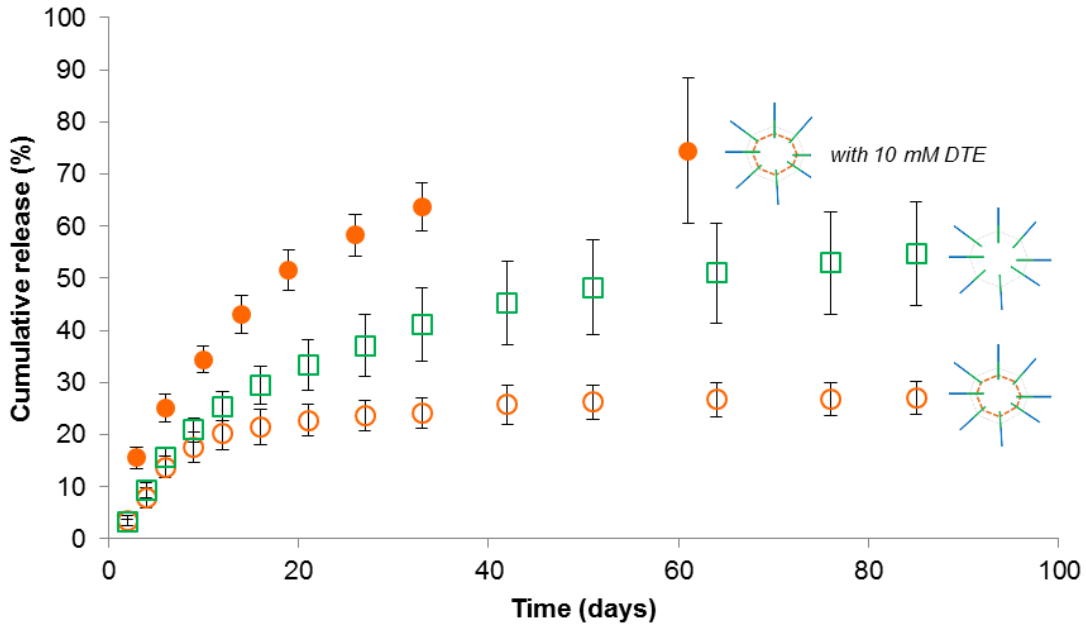

Figure 6. Curcumin release from non-*Lx* PEG-P(HPMA-MTB) micelles (green open squares), *Lx* PEG-P(HPMA-MTB) micelles in absence of dithioerythritol (DTE) (orange open circles) and *Lx* PEG-P(HPMA-MTB) micelles in the presence of 10 mM DTE (orange closed circles). Data are expressed as means ± SD and correspond to measurements in triplicate.

Release studies were performed using the dialysis bag method in water at 37 °C. A low amount of Tween 80 (0.1 w/v %) was added to the release medium to facilitate solubilization of the released curcumin in water, as described in previous literature.[26] Also a very low quantity of the physiologically relevant ascorbic acid (0.0015 w/v %) was dissolved in the release medium to avoid degradation of the drug.[27] Figure 6 shows that 55 % of the initially incorporated curcumin is released in 80 days from the non-*Lx* PEG-P(HPMA-MTB) micelles. For *Lx* PEG-P(HPMA-MTB) micelles, a biphasic release behavior was observed in which 20 % curcumin was released in a similar profile as observed for non-*Lx* PEG-P(HPMA-MTB) micelles during the first 20 days, after which curcumin release leveled off and increased only up to 30 % at day 80. This observed profile suggests that the major fraction of curcumin

is retained better in the *Lx* PEG-P(HPMA-MTB) micelles as compared to non-*Lx* PEG-P(HPMA-MTB) micelles, which can be explained by the *Lx* mediated coordinative core-crosslinking as it prevents destabilization of the micelle and hence premature drug release. The release from *Lx* PEG-P(HPMA-MTB) micelles is comparable to the curcumin release from previously reported PEG-P(HPMA-Bz) micelles containing a long P(HPMA-Bz) block (16 kg/mol), in which a similar high degree of core-crosslinking was facilitated via hydrophobic interactions and π-π stacking effects.[35]

To corroborate that *Lx*-based crosslinking was involved in the drug retention, we modulated the release from *Lx* PEG-P(HPMA-MTB) micelles by adding a coordination-bond disrupting agent to the release medium. The tripeptide glutathione (GSH) is the most abundant reducing agent in mammalian cells having an intracellular concentration in the range of 2 to 10 mM, approximately 100 to 1000 fold higher than its concentration in the extracellular environment (2-20 μM). Tumor cells have at least a 4-fold higher concentration of GSH as compared to normal cells, making GSH-sensitive micelles very attractive for tumor specific intracellular delivery. Apart from its reducing activity, GSH is also a good platinum coordinating ligand by virtue of its free thiol group.[39] Because of the limited stability and activity of GSH under aerobic conditions, we selected the reducing agent dithioerythritol (DTE), the *cis* isomer of 2,3-dihydroxy-1,4-dithiolbutane (Cleland's reagent) as *Lx*-MTB disrupting agent. In the presence of 10 mM DTE, the release from *Lx* PEG-P(HPMA-MTB) micelles was significantly increased as compared to release from *Lx* PEG-P(HPMA-MTB) micelles in the absence of DTE and faster than the release from non-*Lx* PEG-P(HPMA-MTB) micelles (Figure 6). Since the thiol group on DTE is a better ligand for platinum than the thioether group on PEG-P(HPMA-MTB) and since DTE is present in excess, DTE can break existing coordinative bonds, destabilize the micelle and induce drug release. *In vivo* it is expected that the excellent drug retention capability of the *Lx* PEG-P(HPMA-MTB) micelles will lead to little premature drug release in circulation, whereas their small size may result in efficient accumulation in tumor tissue via the EPR effect.[40] In view of the demonstrated possibility of competitive coordination by DTE, it is hypothesized that the micelles are destabilized in the cytoplasm after competitive glutathione displacement, resulting in drug release and tumor cell death. After release

of the payload, it is anticipated that the polymers can be excreted from the body via the renal pathway. Due to hydrolysis of the ester groups connecting the side groups and the main chain, PEG-P(HPMA) will likely be formed, as demonstrated for micelle-forming PEG-P(HPMA) block copolymers in which the P(HPMA) block was functionalized with oligolactates.[32] Since PEG and P(HPMA) are also connected via a hydrolysable ester bond, this may result in the formation of P(HPMA) and PEG. Although these polymers as such are non-degradable, elimination via the kidneys is possible *in vivo* because their molecular weights (5000 and 1300 g/mol, respectively) are below the renal thresholds.[41, 42]

In vitro cell experiments

The cytotoxicity of empty and curcumin-loaded micelles was tested against the breast cancer cell line MCF-7. All tests were performed with associated controls to confirm the non-toxicity of various culture media used in the cytotoxicity experiments. In particular, the effect of 0.1% of DMSO as a co-solvent in the culture medium to ensure the solubility of free curcumin was assessed in accordance with recent work of our group.[43] Also the effect of a slight dilution of the cell culture medium with water was tested as the micellar formulations were prepared in distilled water prior to the cell experiments. All media showed no toxicity (data not shown). It follows from Figure S8 that unloaded *Lx* PEG-P(HPMA-MTB) micelles show almost no cytotoxicity towards MCF-7 cells after 24 hours. The very low level of cytotoxicity may be explained by the presence of the platinum based linker, as unloaded non-*Lx* PEG-P(HPMA-MTB) micelles showed no cytotoxicity after 24 h. A similar slight cytotoxic effect of metal ions was found for PEG-PEI-PCL micelles which were core-crosslinked via coordination between Cu^{2+} ions and the amino groups in the PEI block.[9] Our experiments with unloaded micelles were performed using similar polymer concentrations as those employed in the experiments involving curcumin-loaded non-*Lx* and *Lx* PEG-P(HPMA-MTB) micelles (vide supra), namely 0.03 w/v % for non-*Lx* PEG-P(HPMA-MTB) micelles (i.e. the critical micelle concentration) and 0.14 w/v % for *Lx* PEG-P(HPMA-MTB) micelles. The higher polymer concentration may also be responsible for the slightly higher cytotoxicity of the unloaded *Lx* PEG-P(HPMA-MTB) micelles.

Following these results, we subsequently tested the cytotoxicity of curcumin-loaded micelles against MCF-7 cells. In a first set of experiments, we studied the solubilizing capacity of *Lx* PEG-P(HPMA-MTB) micelles and its effects on cell viability at the lowest possible polymer concentration, i.e. at the CMC (0.009 w/v %). Figure 7 shows that a 0.03 µg/ml solution of curcumin in cell medium (which was prepared by diluting a saturated aqueous curcumin solution) does not induce a significant reduction in MCF-7 cell viability, reflecting the poor solubility of curcumin in water. In contrast, the hydrophobic core of the *Lx* PEG-P(HPMA-MTB) micelles allows for a higher concentration of curcumin (set at 8 µg/ml in these experiments), resulting in a significant decrease in cell viability (4 % cells remaining after 72 h). The curcumin concentration of 8 µg/ml was selected based on our previous research,[43] in which free curcumin (co-solubilized in cell medium by DMSO) showed an intermediate toxicity (ca. 50 %) at this concentration. Figure S9 shows that curcumin is present intracellularly 90 min after treatment of MCF-7 cells with curcumin-loaded *Lx* PEG-P(HPMA-MTB) micelles. Since the curcumin release is still negligible at these early time points (Figure 6), the results suggest that the *Lx* PEG-P(HPMA-MTB) micelles are internalized and intracellularly destabilized, resulting in curcumin release and cell death. The curcumin-loaded *Lx* PEG-P(HPMA-MTB) micellar formulation is more cytotoxic than free curcumin (8 µg/ml) which was solubilized with the help of 0.1% DMSO as a co-solvent (20 % cell viability remaining after 72 h, Figure 7). One should also note that besides being less cytotoxic, free curcumin delivery using DMSO as a co-solvent, although useful as *in vitro* control, is not a realistic formulation for *in vivo* delivery, which further demonstrates the advantage of the *Lx* PEG-P(HPMA-MTB) micellar formulation.

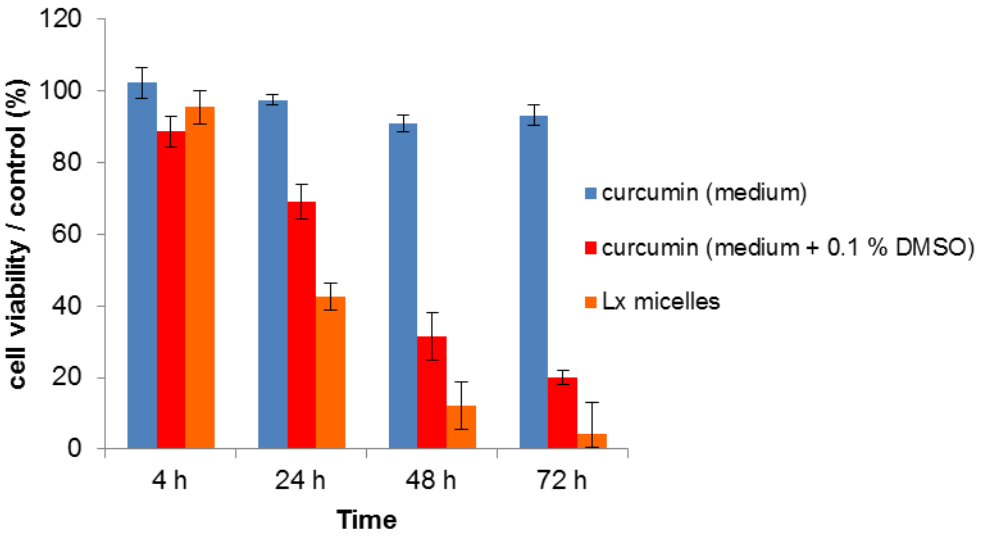

Figure 7. Viability of MCF-7 cells after treatment with an aqueous solution of curcumin (0.03 µg/ml in cell medium) (blue), a solution of curcumin (8 µg/ml) in cell medium containing 0.1 % DMSO (red) and curcumin-loaded (8 µg/ml) *Lx* PEG-P(HPMA-MTB) micelles (orange). Data are expressed as means ± SD and correspond to measurements in quadruplicate. The viability of cells without any treatment (growth medium only) was taken as 100 %.

In a subsequent experiment, we compared the cytotoxicity of non-*Lx* and *Lx* PEG-P(HPMA-MTB) micelles at the CMC of non-*Lx* PEG-P(HPMA-MTB) micelles (0.03 w/v %). A higher curcumin concentration was used in these experiments due to the higher CMC of non-*Lx* PEG-P(HPMA-MTB) micelles compared to *Lx* PEG-P(HPMA-MTB) micelles. At a concentration of 50 µg/ml, non-*Lx* PEG-P(HPMA-MTB) micelles and *Lx* PEG-P(HPMA-MTB) micelles are able to induce almost full cell death within 6 hours (Figure 8). No significant differences between the two micellar formulations are observed in terms of cytotoxicity. In view of the low curcumin release at early timepoints (Figure 6) and the intracellular presence of curcumin 90 min after treatment (Figure S9) it is likely that both types of micelles are internalized and subsequently destabilized. Although at long timescales a clear difference in curcumin release behavior is observed *in vitro* between non-*Lx* and *Lx* PEG-P(HPMA-MTB) micelles (Figure 6), the intracellular micellar destabilization presumably occurs at the same rate for both

formulations, resulting in similar cytotoxic effects. This result, in view of the better curcumin retention capacity of *Lx* PEG-P(HPMA-MTB) micelles (Figure 6), confirms that intracellular competitive coordination occurs for *Lx* PEG-P(HPMA-MTB) micelles, which allows similar release for both systems.

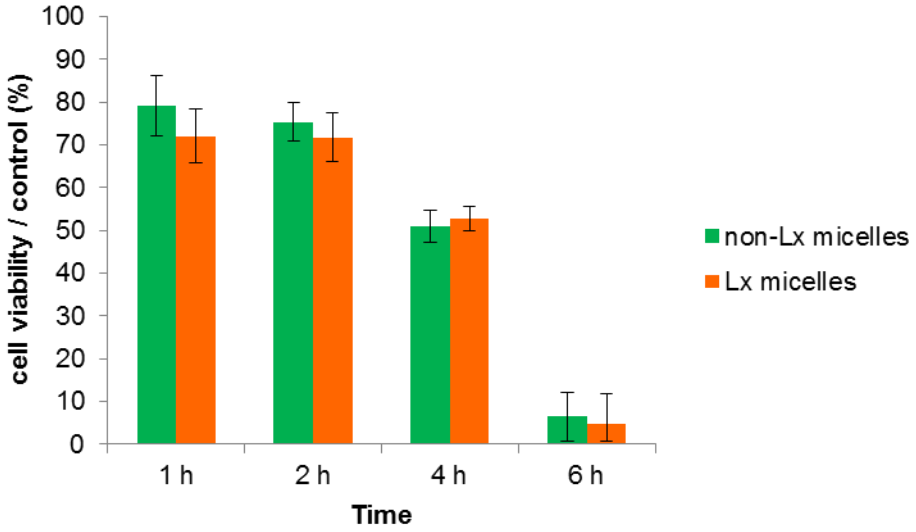

Figure 8. Viability of MCF-7 cells after treatment with curcumin-loaded non-*Lx* PEG-P(HPMA-MTB) micelles (green) and curcumin-loaded *Lx* PEG-P(HPMA-MTB) micelles (orange). The curcumin concentration was 50 µg/ml for both formulations. Data are expressed as means ± SD and correspond to measurements in quadruplicate. The viability of cells without any treatment (growth medium only) was taken as 100 %.

In addition, it is noteworthy that although non-*Lx* and *Lx* PEG-P(HPMA-MTB) micelles exhibit a similar *in vitro* cytotoxicity in this experimental set-up, *Lx* PEG-P(HPMA-MTB) micelles present several advantages regarding the formulation and release of drugs. To mention, *Lx* PEG-P(HPMA-MTB) micelles allow for a lower polymer dose to reach the CMC for the encapsulation of drugs. Furthermore, *Lx* PEG-P(HPMA-MTB) micelles show a better extracellular retention of curcumin in the absence of competitive intracellular ligands in comparison with non-*Lx* PEG-P(HPMA-MTB) micelles

thanks to increased stability via coordinative core-crosslinking. Whereas the above experiments were performed with an unmodified drug, currently investigations are underway involving drug-*Lx* conjugates, which contain a coordination bond between the drug molecule and the platinum atom of *Lx*, as previously reported for drug-*Lx*-antibody conjugates[19, 20] and drug-*Lx*-polymer conjugates.[21] The conjugates can potentially be loaded in high amounts in PEG-P(HPMA-MTB) micelles because of the possibility for coordinative bond formation between drug-*Lx* and a pendant thioether group on PEG-P(HPMA-MTB). The expected synergistic effects of i) a high drug loading, ii) the small size of *Lx* PEG-P(HPMA-MTB) micelles and iii) the demonstrated possibility of breaking coordinative bonds intracellularly via competitive displacement may result in a highly cytotoxic effect *in vitro* and *in vivo*.

Conclusions

PEG-PHPMA block copolymers constitute an appealing basis for micelles because of their biocompatibility, non-immunogenicity and the possibility for functionalization of the P(HPMA) block with groups that facilitate core-crosslinking to stabilize the micelle. In this regard, metal-ligand coordination is particularly attractive because of its specificity and reversibility via competitive displacement. In our present contribution, we combined for the first time these 2 promising concepts by synthesizing PEG-P(HPMA) block copolymers with 4-(methylthio)benzoyl (MTB) side groups that stabilize the micellar core via coordinative crosslinking. As crosslinker we used the platinum-organic *Lx* linker, which has been used for the conjugation of drug molecules to a number of synthetic or natural carriers, but never for the crosslinking and stabilization of micelles. Compared to non-*Lx* PEG-P(HPMA-MTB) micelles, *Lx* PEG-P(HPMA-MTB) micelles exhibited a 3-fold lower CMC and a 3-fold smaller D_H of 60 nm, which is an important property in view of *in vivo* tumor targeting. The *Lx* mediated coordinative core-crosslinking was further confirmed by ^{195}Pt NMR spectroscopy. Although suffering from a limited encapsulation efficiency, the *Lx* PEG-P(HPMA-MTB) micelles showed a better retention of the versatile, hydrophobic drug curcumin during *in vitro* release experiments in comparison with non-*Lx* PEG-P(HPMA-MTB) micelles. When the reducing agent DTE was added, the release of

curcumin from *Lx* PEG-P(HPMA-MTB) micelles was significantly accelerated due to competitive coordination of the platinum atom in *Lx* with DTE, resulting in micellar destabilization. As opposed to previously reported P(HPMA) based micelles,[44-46] *Lx* PEG-P(HPMA-MTB) micelles therefore offer the possibility for a stimulus-responsive drug release. These results confirm our hypothesis that platinum-mediated coordinative micellar core-crosslinking of PEG-P(HPMA-MTB) leads to enhanced micellar stability and stimulus-responsive drug delivery. The combination of a small size, a high stability under normal conditions and a fast drug release under conditions mimicking the intracellular environment make the *Lx* PEG-P(HPMA-MTB) micelles promising materials in the field of nanomedicine. Future work should include optimization of the encapsulation efficiency of the *Lx* PEG-P(HPMA-MTB) micelles, investigation of the cellular uptake route as well as evaluation of the therapeutic efficacy of drug-loaded *Lx* PEG-P(HPMA-MTB) micelles *in vivo*.

Conflicts of interest

Declarations of interest: none.

Acknowledgements

This work was supported by a Marie Skłodowska-Curie Individual Fellowship to S.J.B. in the framework of the 'Horizon 2020' European Union Research and Innovation programme (grant #660953 '*Lx* micelles'). Stéphane Dejean (Department of Artificial Biopolymers, IBMM, Montpellier) and Franck Godiard (Platform for Electron and Analytical Microscopy, Montpellier University) are kindly acknowledged for help with the ^{1}H NMR and TEM experiments, respectively.

References

1. Kwon, G. S.; Kataoka, K. Block copolymer micelles as long-circulating drug vehicles. *Adv. Drug Delivery Rev.* **2012***, 64,* 237-245.

2. Talelli, M.; Barz, M.; Rijcken, C. J. F.; Kiessling, F.; Hennink, W. E.; Lammers, T. Core-crosslinked polymeric micelles: Principles, preparation, biomedical applications and clinical translation. *Nano Today* **2015***, 10*, 93-117.

3. Mahon, E.; Salvati, A.; Baldelli Bombelli, F.; Lynch, I.; Dawson, K. A. Designing the nanoparticle-biomolecule interface for "targeting and therapeutic delivery". *J. Controlled Release* **2012***, 161*, 164-174.

4. Hamad, I.; Hunter, A. C.; Szebeni, J.; Moghimi, S. M. Poly(ethylene glycol)s generate complement activation products in human serum through increased alternative pathway turnover and a MASP-2-dependent process. *Mol. Immunol.* **2008***, 46*, 225-232.

5. Alexis, F.; Pridgen, E.; Molnar, L. K.; Farokhzad, O. C. Factors affecting the clearance and biodistribution of polymeric nanoparticles. *Mol. Pharmaceutics* **2008***, 5*, 505-515.

6. Shi, Y.; Lammers, T.; Storm, G.; Hennink, W. E. Physico-chemical strategies to enhance stability and drug retention of polymeric micelles for tumor-targeted drug delivery. *Macromol. Biosci.* **2017**, *17*, 1600160.

7. Xin, K.; Li, M.; Lu, D.; Meng, X.; Deng, J.; Kong, D.; Ding, D.; Wang, Z.; Zhao, Y. Bioinspired coordination micelles integrating high stability, triggered cargo release, and magnetic resonance imaging. *ACS Appl. Mater. Interfaces* **2017***, 9*, 80-91.

8. Ren, R., Wang, Y., Sun, W. Design, synthesis, characterization and magnetic studies of the metal-quinolate PHEMA-b-HQ polymer micelles. *React. Funct. Polym.* **2016**, *106*, 57-61.

9. Dai, Y.; Zhang, X.; Zhuo, R. Polymeric micelles stabilized by polyethylenimine-copper (C2H5N-Cu) coordination for sustained drug release. *RSC Adv.* **2016***, 6*, 22964-22968.

10. Cao, W.; Li, Y.; Yi, Y.; Ji, S.; Zeng, L.; Sun, Z.; Xu, H. Coordination-responsive selenium-containing polymer micelles for controlled drug release. *Chem. Sci.* **2012***, 3*, 3403-3408.

11. Cao, W., Gu, Y., Meineck, M., Li, T., Xu, H. Tellurium-containing polymer micelles: Competitive-ligand-regulated coordination responsive systems. *JACS* **2014**, *136*, 5132−5137.

12. Talelli, M.; Rijcken, C. J. F.; van Nostrum, C. F.; Storm, G.; Hennink, W. E. Micelles based on HPMA copolymers. *Adv. Drug Delivery Rev.* **2010**, *62*, 231-239.

13. Soga, O.; van Nostrum, C. F.; Fens, M.; Rijcken, C. J. F.; Schiffelers, R. M.; Storm, G.; Hennink, W. E. Thermosensitive and biodegradable polymeric micelles for paclitaxel delivery. *J. Controlled Release* **2005***, 103*, 341-353.

14. Shi, Y.; Van Steenbergen, M. J.; Teunissen, E. A.; Novo, L.; Gradmann, S.; Baldus, M.; Van Nostrum, C. F.; Hennink, W. E. Π-Π stacking increases the stability and loading capacity of thermosensitive polymeric micelles for chemotherapeutic drugs. *Biomacromolecules* **2013***, 14*, 1826-1837.

15. Shi, Y.; Cardoso, R. M.; Van Nostrum, C. F.; Hennink, W. E. Anthracene functionalized thermosensitive and UV-crosslinkable polymeric micelles. *Polym. Chem.* **2015***, 6*, 2048-2053.

16. Kasmi, S.; Louage, B.; Nuhn, L.; Van Driessche, A.; Van Deun, J.; Karalic, I.; Risseeuw, M.; Van Calenbergh, S.; Hoogenboom, R.; De Rycke, R. Transiently responsive block copolymer micelles based on N-(2-hydroxypropyl) methacrylamide engineered with hydrolyzable ethylcarbonate side chains. *Biomacromolecules* **2015***, 17*, 119-127.

17. Wei, R.; Cheng, L.; Zheng, M.; Cheng, R.; Meng, F.; Deng, C.; Zhong, Z. Reduction-responsive disassemblable core-cross-linked micelles based on poly(ethylene glycol)-b-poly(N-2-hydroxypropyl methacrylamide)-lipoic acid conjugates for triggered intracellular anticancer drug release. *Biomacromolecules* **2012***, 13*, 2429-2438.

18. Shi, Y.; Van Der Meel, R.; Theek, B.; Oude Blenke, E.; Pieters, E. H.; Fens, M. H.; Ehling, J.; Schiffelers, R. M.; Storm, G.; Van Nostrum, C. F. Complete regression of xenograft tumors upon

targeted delivery of paclitaxel via Π-Π stacking stabilized polymeric micelles. *ACS Nano* **2015***, 9*, 3740-3752.

19. Sijbrandi, N. J.; Merkul, E.; Muns, J. A.; Waalboer, D. C.; Adamzek, K.; Bolijn, M.; Montserrat, V.; Somsen, G. W.; Haselberg, R.; Steverink, P. J.; Houthoff, H. J.; van Dongen, G. A. A novel platinum(II)-based bifunctional ADC linker benchmarked using 89Zr-desferal and auristatin F-conjugated trastuzumab. *Cancer Res.* **2017***, 77*, 257-267.

20. Waalboer, D. C. J.; Muns, J. A.; Sijbrandi, N. J.; Schasfoort, R. B. M.; Haselberg, R.; Somsen, G. W.; Houthoff, H.; van Dongen, G. A. M. S. Platinum(II) as bifunctional linker in antibody-drug conjugate formation: Coupling of a 4-nitrobenzo-2-oxa-1,3-diazole fluorophore to trastuzumab as a model. *ChemMedChem* **2015***, 10*, 797-803.

21. Dolman, M. E. E. M.; van Dorenmalen, K. M. A.; Pieters, E. H. E.; Sparidans, R. W.; Lacombe, M.; Szokol, B.; Orfi, L.; Kéri, G.; Bovenschen, N.; Storm, G.; Hennink, W. E.; Kok, R. J. Dendrimer-based macromolecular conjugate for the kidney-directed delivery of a multitargeted sunitinib analogue. *Macromol. Biosci.* **2012***, 12*, 93-103.

22. Dolman, M. E. M.; Fretz, M. M.; Segers, G. J. W.; Lacombe, M.; Prakash, J.; Storm, G.; Hennink, W. E.; Kok, R. J. Renal targeting of kinase inhibitors. *Int. J. Pharm.* **2008***, 364*, 249-257.

23. Ulbrich, K.; Šubr, V.; Strohalm, J.; Plocova, D.; Jelınková, M.; Říhová, B. Polymeric drugs based on conjugates of synthetic and natural macromolecules: I. Synthesis and physico-chemical characterisation. *J. Controlled Release* **2000***, 64*, 63-79.

24. Wu, H.; Yang, Y.; Cao, Y. C. Synthesis of colloidal uranium-dioxide nanocrystals. *J. Am. Chem. Soc.* **2006***, 128*, 16522-16523.

25. Neradovic, D.; Van Nostrum, C. F.; Hennink, W. E. Thermoresponsive polymeric micelles with controlled instability based on hydrolytically sensitive N-isopropylacrylamide copolymers. *Macromolecules* **2001***, 34*, 7589-7591.

26. Gao, X.; Zheng, F.; Guo, G.; Liu, X.; Fan, R.; Qian, Z.; Huang, N.; Wei, Y. Improving the anti-colon cancer activity of curcumin with biodegradable nano-micelles. *J. Mater. Chem. B* **2013***, 1*, 5778-5790.

27. Wang, Y.; Pan, M.; Cheng, A.; Lin, L.; Ho, Y.; Hsieh, C.; Lin, J. Stability of curcumin in buffer solutions and characterization of its degradation products. *J. Pharm. Biomed. Anal.* **1997***, 15*, 1867-1876.

28. Fliervoet, L. A. L., Najafi, M., Hembury, M., Vermonden, T. Heterofunctional poly(ethylene glycol) (PEG) macroinitiator enabling controlled synthesis of ABC triblock copolymers. *Macromolecules* **2017**, *50*, 8390-8397.

29. Shi, Y., Kunjachan, S., Wu, Z., Gremse, F., Moeckel, D., Van Zandvoort, M., Kiessling, F., Storm, G., Van Nostrum, C. F., Hennink, W. E., Lammers, T. Fluorophore labeling of core-crosslinked polymeric micelles for multimodal in vivo and ex vivo optical imaging. *Nanomedicine* **2015**, *10*, 1111–1125.

30. Stenzel, M. H. RAFT polymerization: an avenue to functional polymeric micelles for drug delivery. *Chem. Commun.* **2008**, 3486–3503.

31. Matyjaszewski, K. Atom transfer radical polymerization (ATRP): Current status and future perspectives. *Macromolecules* **2012**, *45*, 4015–4039.

32. Soga, O.; Van Nostrum, C. F.; Ramzi, A.; Visser, T.; Soulimani, F.; Frederik, P. M.; Bomans, P. H. H.; Hennink, W. E. Physicochemical characterization of degradable thermosensitive polymeric micelles. *Langmuir* **2004**, *20*, 9388-9395.

33. Du, N., Guo, W., Yu, G., Guan, S., Guo, L., Shen, T., Tang H., Gan, Z. Poly(D,L-lactic acid)-block-poly(N-(2-hydroxypropyl)methacrylamide) nanoparticles for overcoming accelerated blood clearance and achieving efficient anti-tumor therapy. *Polym. Chem.* **2016**, *7*, 5719-5729.

34. Chaudhary, A. K., Lopez, J., Beckman, E. J., Russell, A. J. Biocatalytic solvent-free polymerization to produce high molecular weight polyesters. *Biotechnol. Prog.* **1997**, *13*, 318-325.

35. Naksuriya, O.; Shi, Y.; van Nostrum, C. F.; Anuchapreeda, S.; Hennink, W. E.; Okonogi, S. HPMA-based polymeric micelles for curcumin solubilization and inhibition of cancer cell growth. *Eur. J. Pharm. Biopharm.* **2015***, 94*, 501-512.

36. Oehlsen, M. E.; Qu, Y.; Farrell, N. Reaction of polynuclear platinum antitumor compounds with reduced glutathione studied by multinuclear (1H, 1H-15N gradient heteronuclear single-quantum coherence, and 195Pt) NMR spectroscopy. *Inorg. Chem.* **2003***, 42*, 5498-5506.

37. Kasherman, Y.; Sturup, S.; Gibson, D. Trans labilization of am(m)ine ligands from platinum (II) complexes by cancer cell extracts. *JBIC, J. Biol. Inorg. Chem.* **2009***, 14*, 387-399.

38. Song, Z.; Feng, R.; Sun, M.; Guo, C.; Gao, Y.; Li, L.; Zhai, G. Curcumin-loaded PLGA-PEG-PLGA triblock copolymeric micelles: Preparation, pharmacokinetics and distribution in vivo. *J. Colloid Interface Sci.* **2011***, 354*, 116-123.

39. Gonzalo, T.; Talman, E. G.; van de Ven, A.; Temming, K.; Greupink, R.; Beljaars, L.; Reker-Smit, C.; Meijer, D. K. F.; Molema, G.; Poelstra, K.; Kok, R. J. Selective targeting of pentoxifylline to hepatic stellate cells using a novel platinum-based linker technology. *J. Controlled Release* **2006**, *111*, 193-203.

40. Cabral, H.; Matsumoto, Y.; Mizuno, K.; Chen, Q.; Murakami, M.; Kimura, M.; Terada, Y.; Kano, M. R.; Miyazono, K.; Uesaka, M.; Nishiyama, N.; Kataoka, K. Accumulation of sub-100 nm polymeric micelles in poorly permeable tumours depends on size. *Nat. Nanotechnol.* **2011***, 6*, 815-823.

41. Yamaoka, T.; Tabata, Y.; Ikada, Y. Distribution and tissue uptake of poly(ethylene glycol) with different molecular weights after intravenous administration to mice. *J. Pharm. Sci.* **1994***, 83*, 601-606.

42. Seymour, L. W.; Duncan, R.; Strohalm, J.; Kopeček, J. Effect of molecular weight (mw) of N-(2-hydroxypropyl)methacrylamide copolymers on body distribution and rate of excretion after subcutaneous, intraperitoneal, and intravenous administration to rats. *J. Biomed. Mater. Res.* **1987***, 21*, 1341-1358.

43. Al Samad, A.; Bethry, A.; Koziolová, E.; Netopilik, M.; Etrych, T.; Bakkour, Y.; Coudane, J.; El Omar, F.; Nottelet, B. CL-PEG graft copolymers with tunable amphiphilicity as efficient drug delivery systems. *J. Mater. Chem. B* **2016***, 4*, 6228-6239.

44. Sponchioni, M.; Palmiero, U. C.; Moscatelli, D. HPMA-PEG surfmers and their use in stabilizing fully biodegradable polymer nanoparticles. *Macromol. Chem. Phys.* **2017**, *218*, 1700380.

45. Krimmer, S. G.; Pan, H.; Liu, J.; Yang, J.; Kopecek, J. Synthesis and characterization of poly(e-caprolactone)-block-poly[N-(2-hydroxypropyl)methacrylamide] micelles for drug delivery. *Macromol. Biosci.* **2011**, *11*, 1041–1051.

46. Du, N.; Guo, W.; Yu, Q.; Guan, S.; Guo, L.; Shen, T.; Tang, H.; Gan, Z. Poly(D,L-lactic acid)-block-poly(N-(2-hydroxypropyl)methacrylamide) nanoparticles for overcoming accelerated blood clearance and achieving efficient anti-tumor therapy. *Polym. Chem.* **2016**, *7*, 5719–5729.

Supporting information for

Reversibly core-crosslinked PEG-P(HPMA) micelles: Platinum coordination chemistry for competitive-ligand-regulated drug delivery

Sytze Buwalda,[a] Benjamin Nottelet,[a] Audrey Bethry,[a] Robbert Jan Kok,[b] Niels Sijbrandi,[c] Jean Coudane[a]*

[a] IBMM, Université de Montpellier, CNRS, ENSCM, Faculté de Pharmacie, 15 avenue Charles Flahault, BP14491, 34093 Montpellier cedex 5, France

[b] Department of Pharmaceutics, Utrecht Institute for Pharmaceutical Sciences, Utrecht University, Universiteitsweg 99, 3584 CG Utrecht, The Netherlands

[c] LinXis B.V., Boelelaan 1085c, Amsterdam, 1081 HV, The Netherlands

*Corresponding author. Telephone number: +33(0)4-11-75-96-97; Fax number: +33(0)4-11-75-97-28

E-mail addresses: sijtze.buwalda@umontpellier.fr; benjamin.nottelet@umontpellier.fr; audrey.bethry@univ-montp1.fr; r.j.kok@uu.nl; sijbrandi@linxispharmaceuticals.com; jean.coudane@umontpellier.fr

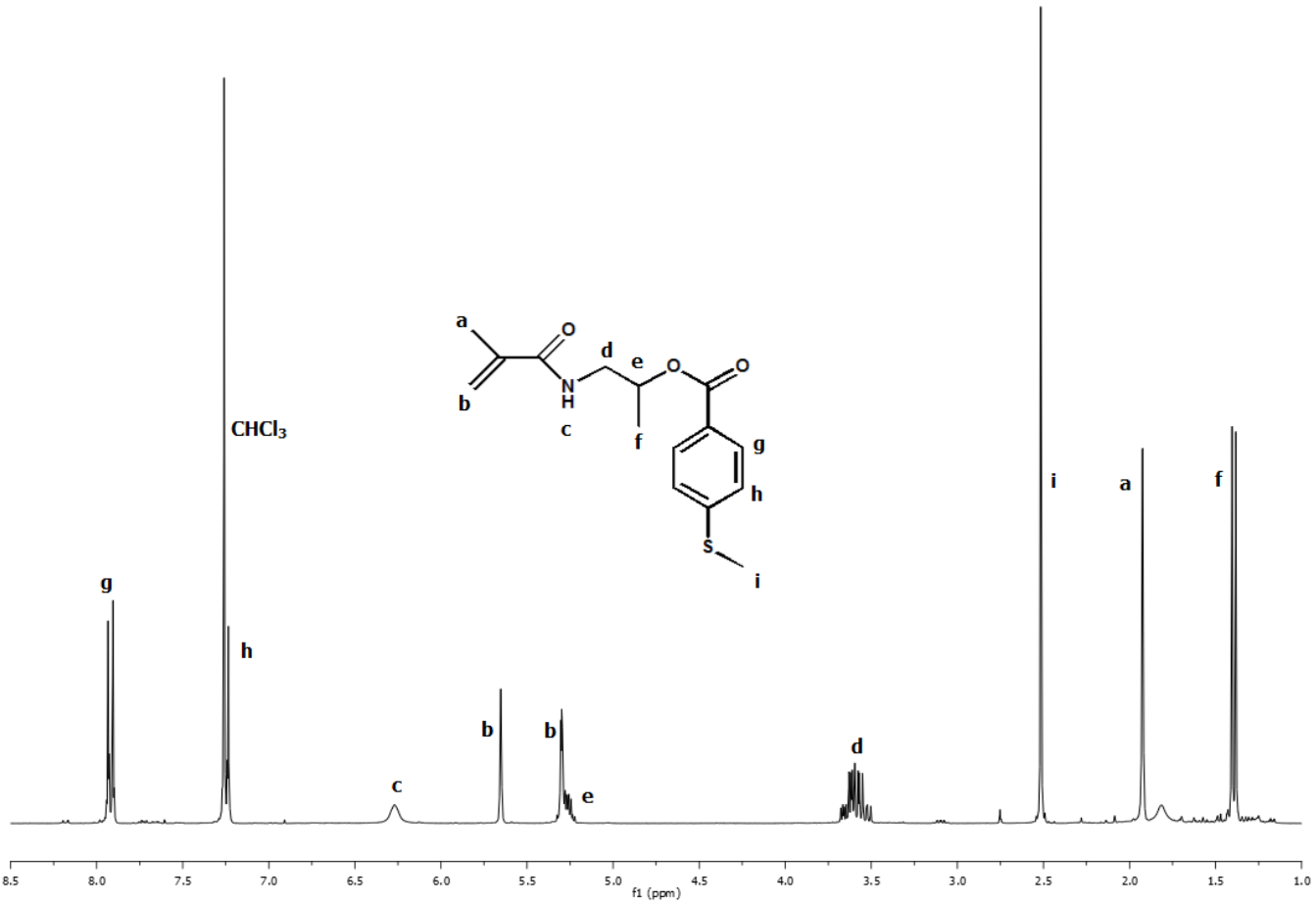

Figure S1. ^{1}H NMR spectrum of N-(2-(4-methylthio)benzoyloxypropyl) methacrylamide (HPMA-MTB). Solvent: $CDCl_3$.

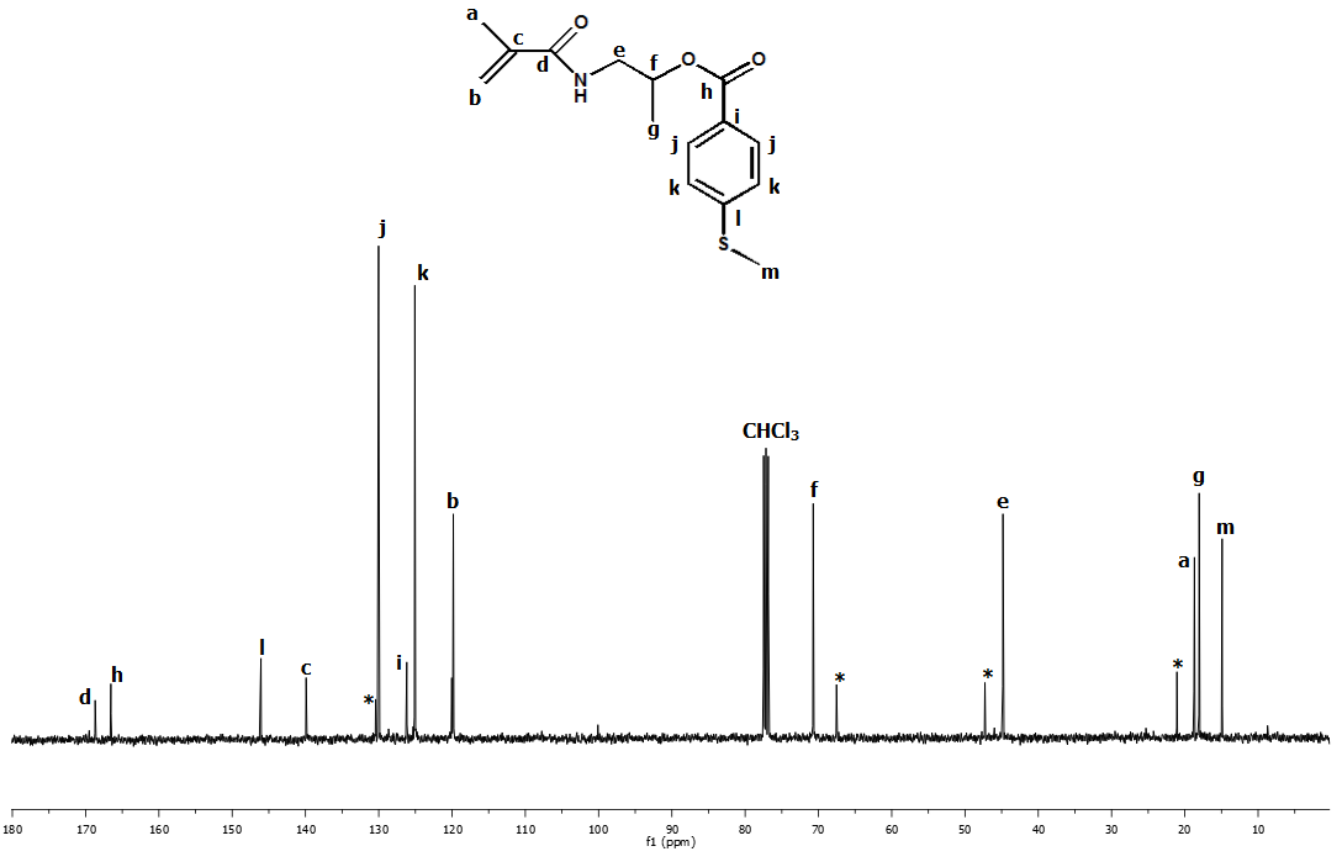

Figure S2. ^{13}C NMR spectrum of N-(2-(4-methylthio)benzoyloxypropyl) methacrylamide (HPMA-MTB). Solvent: $CDCl_3$. The peaks marked with an asterisk (*) relate to impurities, most likely HPMA and MTB that formed after hydrolysis of HPMA-MTB upon long-term storage.

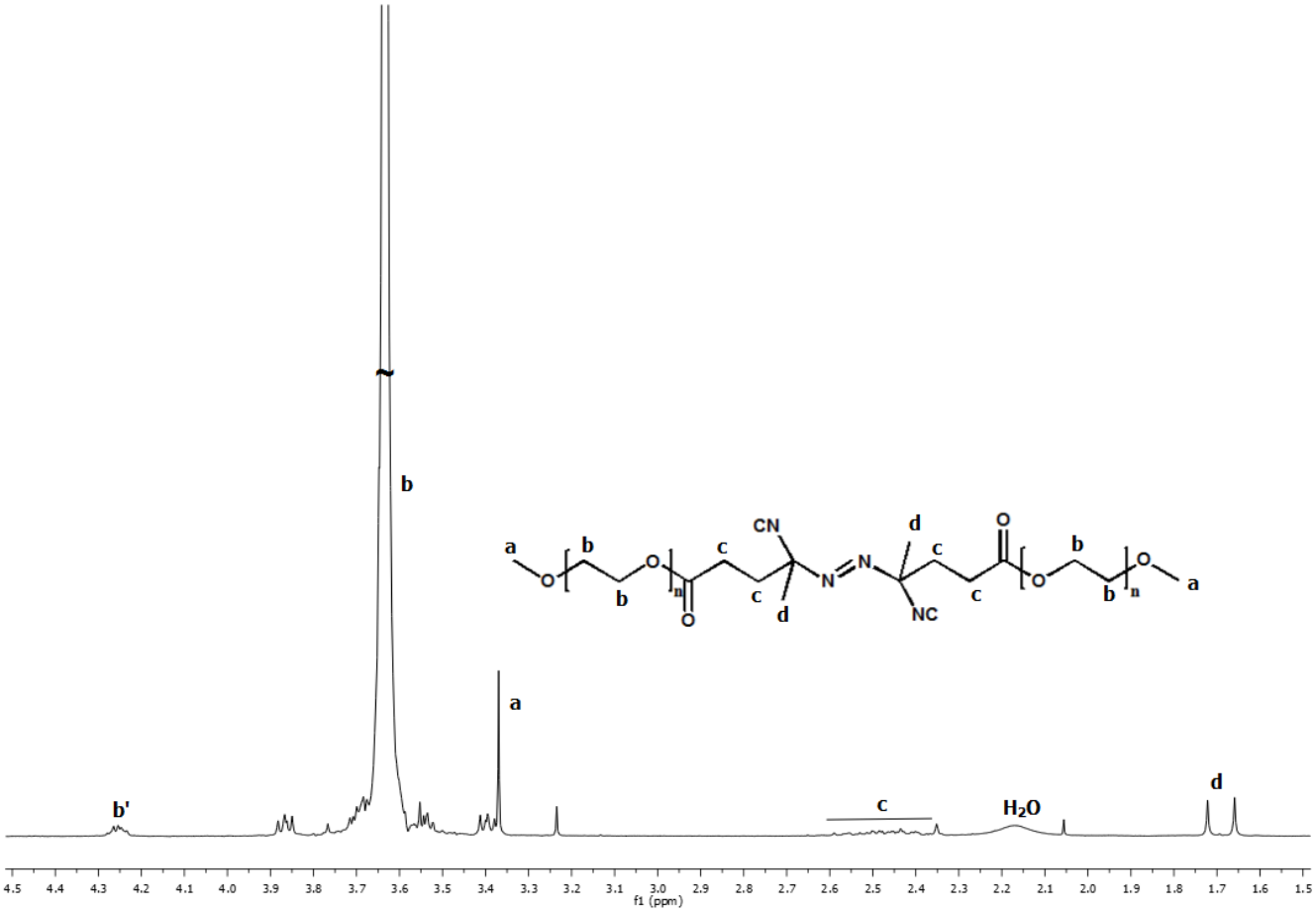

Figure S3. ^{1}H NMR spectrum of $(PEG)_2$-ABCPA macro-initiator. Peak **b'** corresponds to terminal PEG protons. Solvent: $CDCl_3$.

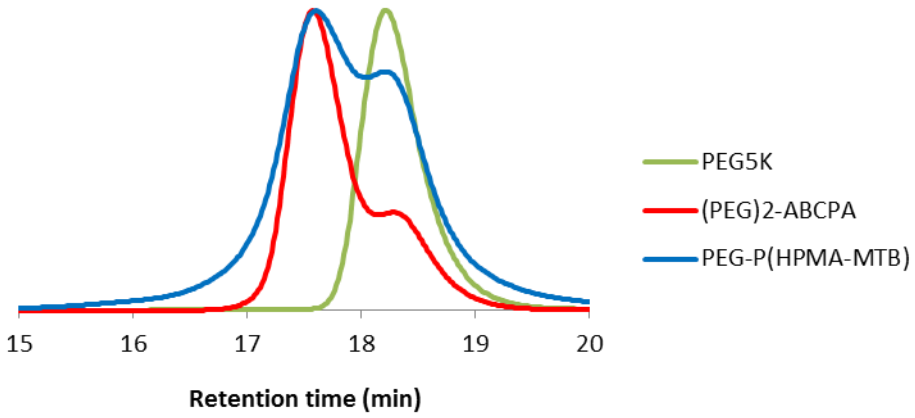

Figure S4. Normalized SEC traces of PEG5K, $(PEG)_2$-ABCPA and PEG-P(HPMA-MTB).

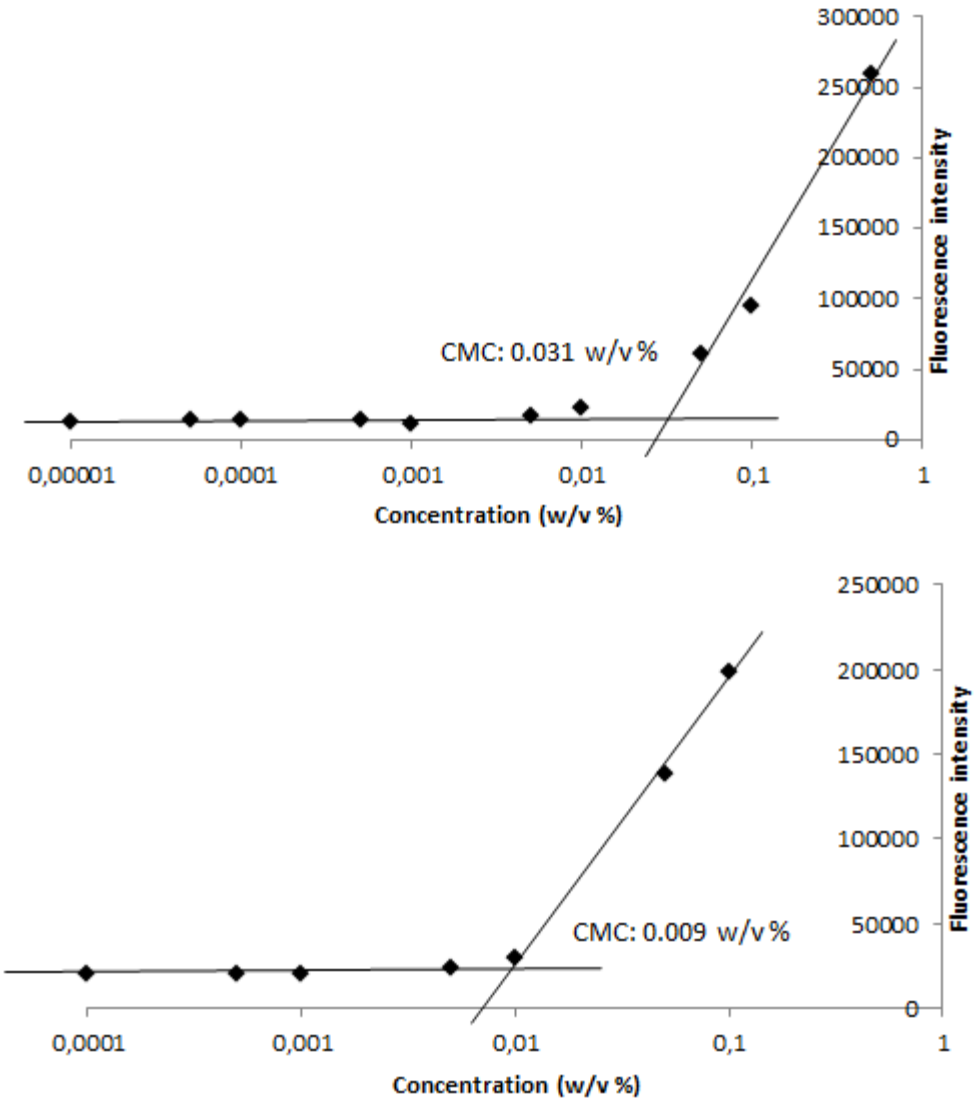

Figure S5. Determination of the critical micelle concentration (CMC) for non-*Lx* PEG-P(HPMA-MTB) micelles (top) and *Lx* PEG-P(HPMA-MTB) micelles (bottom). The concentration at the intersection of the two straight lines corresponds to the CMC.

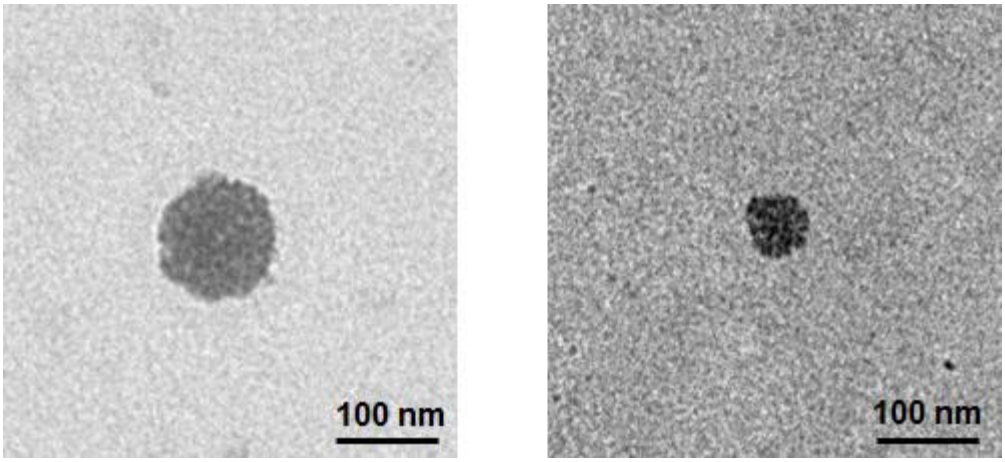

Figure S6. Representative TEM images of a non-*Lx* PEG-P(HPMA-MTB) micelle (left) and a *Lx* PEG-P(HPMA-MTB) micelle (right).

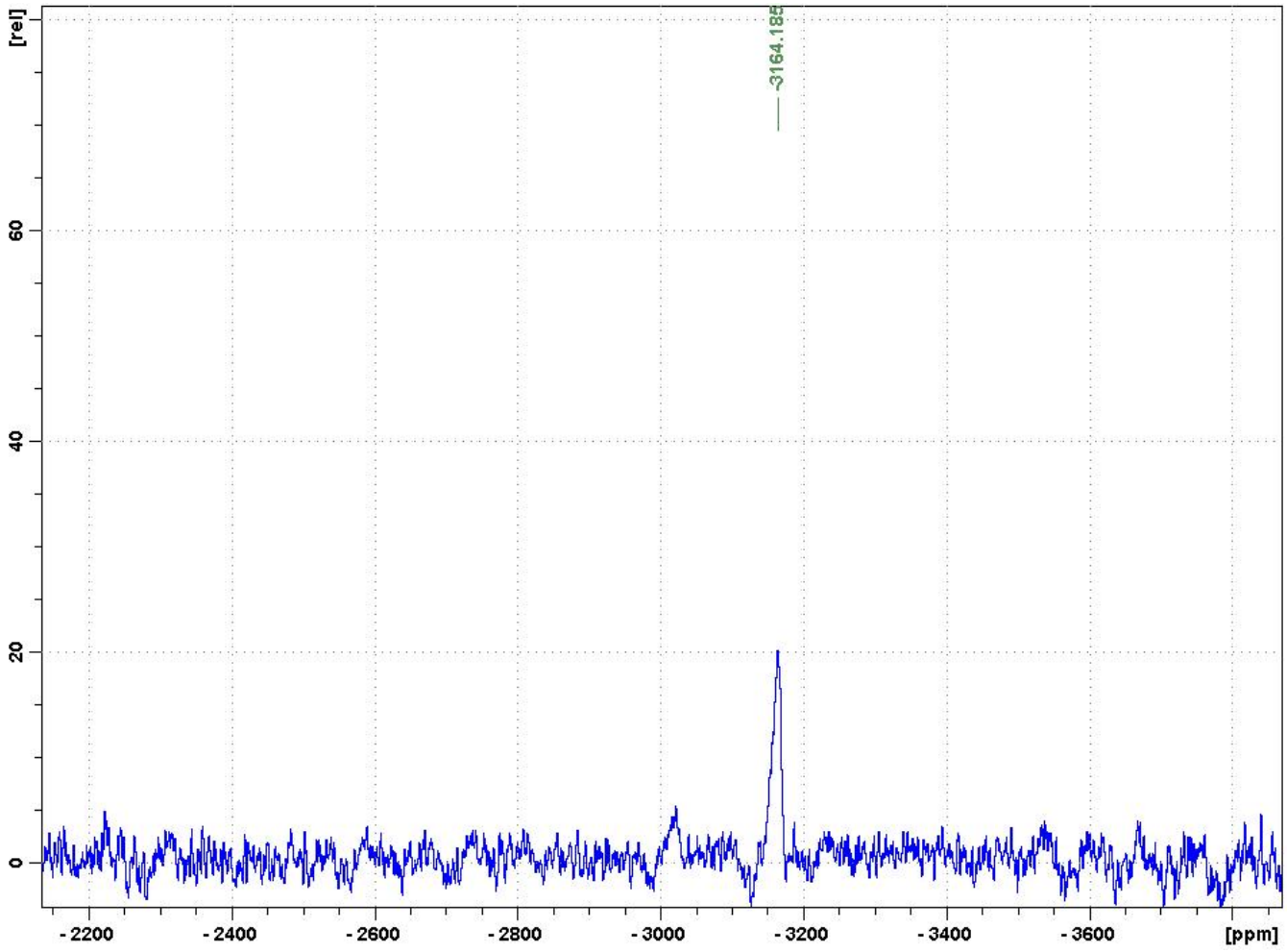

Figure S7. ^{195}Pt NMR spectrum of a *Lx* PEG-P(HPMA-MTB) micellar solution. Solvent: D_2O.

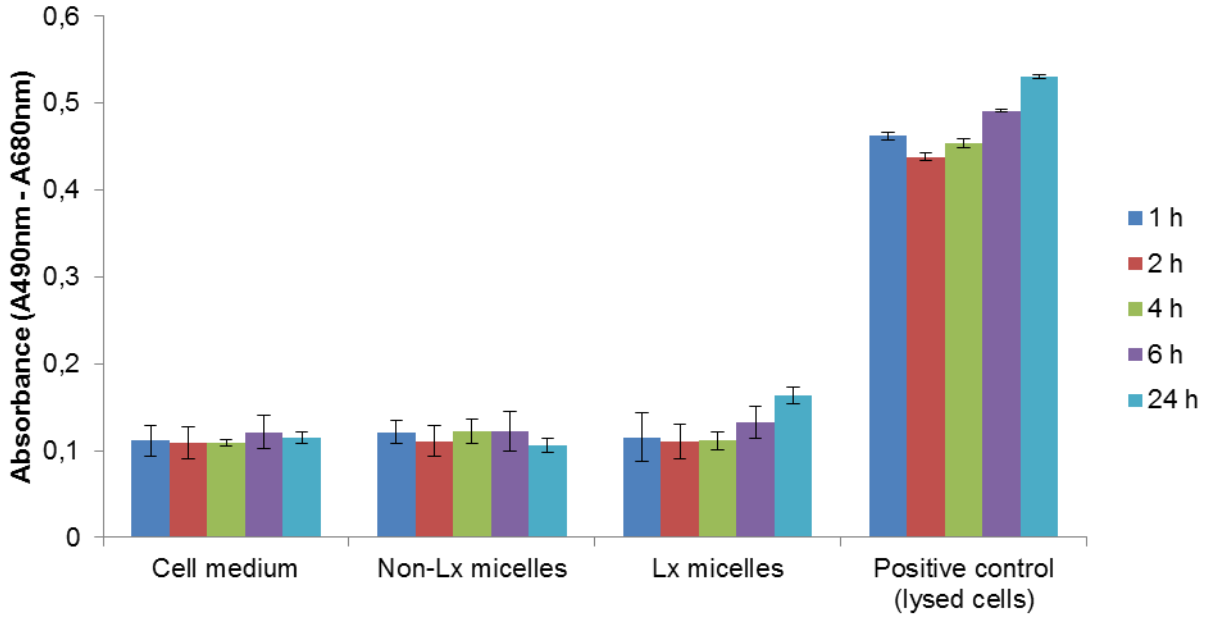

Figure S8. Cytotoxicity of unloaded non-*Lx* PEG-P(HPMA-MTB) and *Lx* PEG-P(HPMA-MTB) micellar formulations (0.03 and 0.14 w/v % in cell medium, respectively). Data (n = 4) are expressed as mean ± standard deviation.

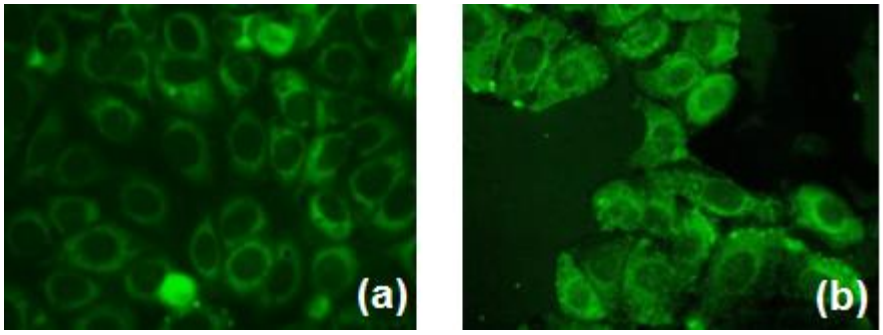

Figure S9. Curcumin-derived green fluorescence in MCF-7 cells after treatment with: (a) curcumin-loaded non-*Lx* PEG-P(HPMA-MTB) micelles, (b) curcumin-loaded *Lx* PEG-P(HPMA-MTB) micelles. The curcumin concentration was 50 μg/ml for both formulations. Images were taken 90 min after treatment using a Leica DM IRB inverted microscope at 40 x magnification.